



# Ecofriendly inclined drilling of carbon fiber-reinforced polymers (CFRP)

Salman Pervaiz<sup>1</sup> · Sathish Kannan<sup>2</sup> · Dehong Huo<sup>3</sup> · Ramulu Mamidala<sup>4</sup>

Received: 3 July 2020 / Accepted: 29 September 2020 / Published online: 23 October 2020  
© The Author(s) 2020

## Abstract

Key composite made aerostructures such as fuselage inner walls, flap support fairings, empennage ribs, and the vertical fin ribs are comprised of non-vertical inclined and radial holes that join with other key metallic and non-metallic structures. Carbon fiber reinforced plastics (CFRP) are also used in the aerospace, automotive, marine, and sports-related applications due to their superior properties such as high strength to weight ratio, better fatigue, and high stiffness. CFRP drilling operation is different than the homogenous materials as the cutting-edge interacts with fiber and matrix simultaneously. Flank face of the tool rubs on the workpiece material and develops high frictional contact due to the elastic recovery of broken fibers. Lubrication during CFRP cutting can reduce the friction involved at tool-workpiece interface to enhance cutting performance. Dry cutting, cryogenic machining, and minimum quantity lubrication (MQL)-based strategies are termed as ecofriendly cooling/lubrication methods when machining high performance materials. The abrasive nature of carbon fiber is responsible of producing cutting forces which leads to different types of imperfections such as delamination, uncut fiber, fiber breakout, and fiber pullout. The integrity of CFRP drilled hole especially at the entry and exit of the hole plays a significant role towards the overall service life. The presented paper aims to characterize the interrelationships between hole inclination, lubrication/cooling methods, tool coating, and drill geometry with inclined hole bore surface quality and integrity during drilling of CFRP laminates. In dry cutting, thrust forces were found 2.38 times higher in the 30° inclination when compared with the reference 90° conventional inclination angle. Compressed air provided lowest increase (1.46 times) in the thrust forces for 30° inclination.

**Keywords** CFRP · Machining · Drilling · MQL · Dry · Compressed-air · Sustainable

## 1 Introduction

Machining operations bear excessive environmental burden due to the involvement of high energy demand, problem with waste water disposal, air borne emissions, and health and safety occupational concerns [1]. Significant portion of the

environmental burden came from the cutting fluid application. Eco-friendly machining has been promoted with respect to the utilization of cutting fluids using different green strategies such as prolonging the life of the cutting fluid, replacing conventional nonbiodegradable cutting fluids with the biodegradable cutting fluids, and replacing conventional high flow rate flood cooling with the lower consumption rate strategies [2]. Dry cutting, cryogenic machining, and minimum quantity lubrication (MQL)-based strategies are termed as ecofriendly cooling/lubrication methods when machining engineering materials [3]. The demand of using CFRP composite is increasing exponentially especially for the aerospace, sports, and automotive sectors due to its favorable properties such as high strength to weight ratio, higher stiffness, and fatigue life. According to a market research report titled “The Aerospace Composites,” by 2022, advanced aircrafts such as the BOEING 787-TEN Dreamliner™ and that of the AIRBUS 400 M military transport aircraft will have more than 50% CFRP composite panels on the airframe. As per the

---

✉ Dehong Huo  
dehong.huo@newcastle.ac.uk

<sup>1</sup> Department of Mechanical Engineering, Rochester Institute of Technology - Dubai Campus, Dubai, United Arab Emirates

<sup>2</sup> Department of Mechanical Engineering, American University of Sharjah, Sharjah, United Arab Emirates

<sup>3</sup> Mechanical Engineering, School of Engineering, Newcastle University, Newcastle upon Tyne NE1 7RU, UK

<sup>4</sup> Department of Mechanical Engineering, University of Washington, Seattle, WA 98195, USA

assembling requirements of CFRP parts, drilling operation is considered as a major processing operation conducted on CFRP products [4]. Major aerostructures such as fuselage inner walls, flap support fairings, empennage ribs, and the vertical fin ribs are comprised of non-vertical inclined and radial holes that join with other key metallic and non-metallic structures. Inclined drilling has potential applications in the industrial sectors mentioned above and can enhance the processing of high-performance composites. Machining of these inclined holes is of utmost importance as they affect the tensile and impact strength of the structures in service. In addition, inclined holes are required to be machined to provide access for electrical wires and hydraulic pipes which can lead to stress concentration points during loading process.

Chip formation in CFRP machining is a function of fiber volume fraction and the type of matrix. They can be powdery or continuous due to these factors. It is also pointed out in literature [5] that flank face of the tool rubs on the workpiece material and develops high frictional contact due to the elastic recovery of broken fibers. Several researchers have focused their research work on the drilling performance of CFRP composites under different lubrication methods. Xia et al. [6] investigated the drilling performance when cutting CFRP composites using cryogenic cooling and dry cutting. The study investigated the influence of cutting-edge radius by monitoring cutting force, torque, delamination factor, and outer corner drill tool wear. The study revealed that drill bit cutting edge corner wear and rounding was reduced; as a result surface integrity of the generated hole was also improved. Ismail et al. [7] in another study investigated the machinability of different types of conventional and sustainable fiber reinforced polymers (FRP) composites. The study investigated the influence of drilling parameters on chip formation and delamination of composite layers. The study utilized high-speed steel (HSS) drill bits under dry cutting conditions. The study revealed that increasing feed rate and thrust force increased delamination and surface roughness. The study recommended optimal performance for feed rate 0.05–0.1 mm/rev and cutting speed of 30 m/min. Brinksmeier and Janssen [8] investigated the drilling performance of multi-layer materials consisting of CFRP, titanium, and aluminum alloys. The study observed cutting forces, hole integrity, tool wear, and chip morphology. The study incorporated conventional and step drills under dry and MQL cooling methods. The study revealed MQL as potential method when drilling multi-layer materials. The study also found that step drill provided better surface integrity, tool life, and dimensional tolerance.

Senthilkumar et al. [9] investigated the drilling performance of CFRP/Ti6Al4V stacks under minimum quantity lubrication technique. The study investigated three different tool geometries with two cutting tool materials such as K20 carbide and TiAlN-coated carbide using various flow rates of LRT 30 oil-based MQL. The study monitored drilling

performance by observing hole profile, burr geometry, thrust force, chip morphology, and tool wear. The study revealed that drill bit with point angle  $135^\circ$  and helix angle  $30^\circ$  provided minimum thrust force and best hole integrity. Merino-Pérez et al. [10] investigated the distribution of cutting temperature in the bore hole when drilling different CFRP material systems. The study utilized uncoated carbide drill bits, and cutting temperature was captured using thermocouples and infrared camera. The study also measured cutting temperature distribution for cutting speed ranging from 50 to 200 m/min. The study revealed that higher concentration of heat was found at higher cutting speeds ranging from 150 to 200 m/min. Meshreki et al. [11] provided a comprehensive study about drilling CFRP/aluminum stacks. These composite stacks are difficult to drill due to poor chip evacuation and material-based heterogeneity. The study utilized four different cooling strategies, namely dry, flood, MQL (low pressure and high flowrate), and MQL (high pressure and low flowrate). The study monitored cutting forces and temperature during the cutting process. Due to the aluminum stacking, CFRP exit hole delamination was not observed. The study revealed that MQL cooling provided entry damage delamination when compared with dry and flood cooling methods. In addition, study found that MQL (high pressure and low flowrate) provided similar hole quality to flood cooling.

Several studies are available in literature where performance of different cutting tool materials is discussed for CFRP drilling process. Swan et al. [15] study the drilling performance of CFRP using uncoated and different coated tools with coatings such as DLC, AlMgB<sub>14</sub>, AlCrN, AlCrSi/TiN, and Si<sub>3</sub>N<sub>4</sub>. The study examined tool wear and related tool wear mechanisms. It was observed that AlCrSi/TiN coating outperformed others in performance. The study linked best performance of coating with the similar stiffness of coating and substrate materials and better adhesion between both materials. Literature points out at many approaches proposing that reduction in thrust force at the outer layers can reduce the delamination and drilling-induced damage. These strategies can be incorporated by specialized variable feed control method, using back plates to support the outer layers, circular milling, and wobble milling. The process of conventional uniaxial drilling of CFRP has been extensively studied in the literature. Cutting is achieved in the drilling process by the combine movements of the chisel edge, the main cutting edge, and minor cutting edge. Literature links drilling-induced delamination of CFRP with the thrust force generated during cutting [16]. This thrust force is further decomposed in the thrust force component due to the cutting lip and thrust force component due to the chisel edge as shown in the schematic illustration in Fig. 1a [12].

Xu et al. [17] investigated the performance of TiAlN and diamond-coated drills using dry and MQL cooling when drilling CFRP/Ti6Al4V stacks. The study revealed that cutting

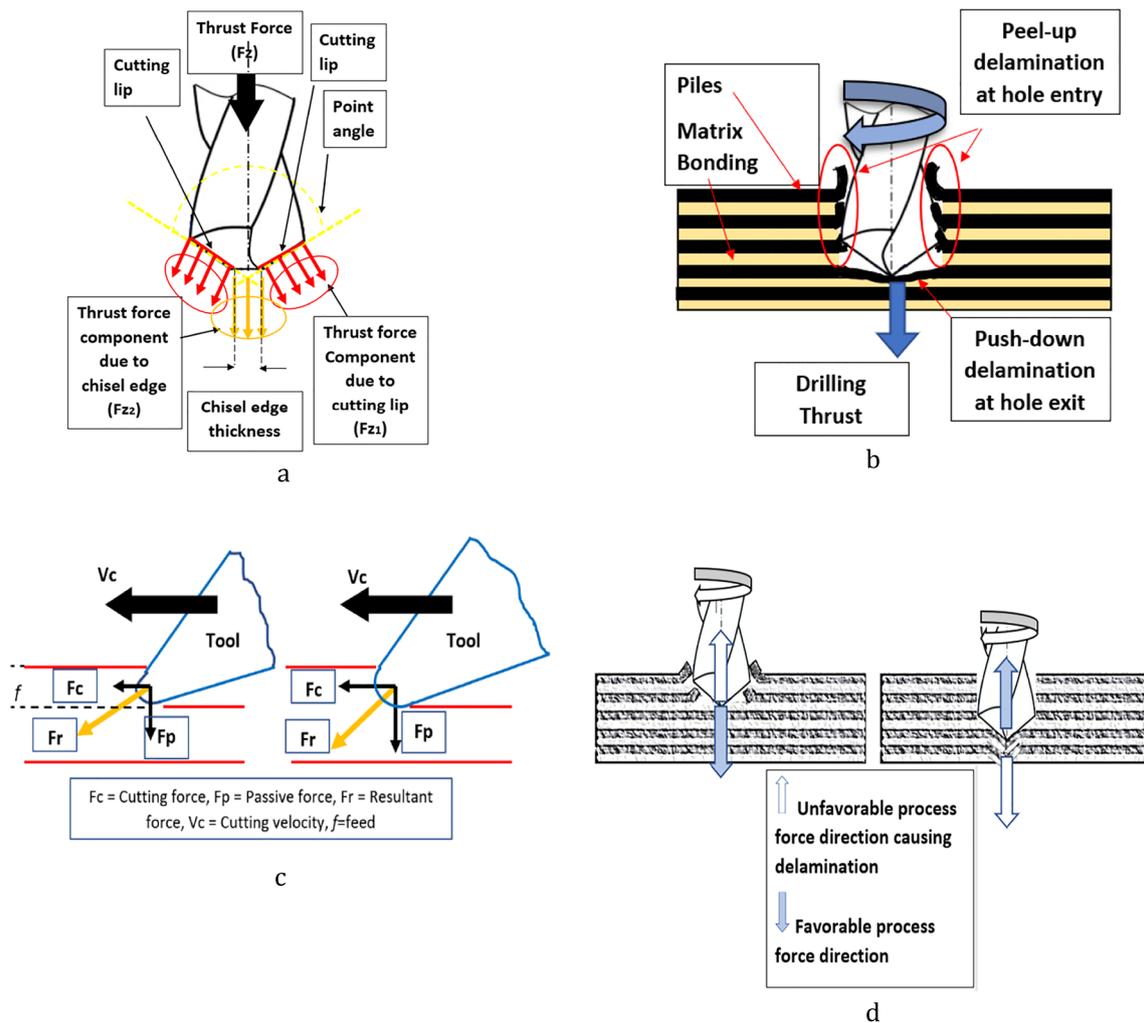


**Fig. 1** a Schematic illustration of thrust force ( $F_z$ ) decomposition into components for cutting lip and chisel edge (adopted from [12]). b Schematic illustration of delamination-based damage of CFRP during

drilling (adopted from [13]). c Schematic illustration of favorable force direction (adopted from [14])

happens below the machined surface and MQL oil has tendency to flow in the surface cavities besides forming a lubrication film. It is also reported that MQL has tendency to moisten the powdery CFRP chips that sticks with cutting tool and increases cutting forces. Xu et al. [18] also compared the drilling performance of carbon-epoxy and carbon-polyamide composites. Thermoset plastic-based carbon-epoxy composite provided higher cutting forces and temperature. Drilling comparison of carbon-polyamide and carbon-Polyetheretherketone shows that carbon/Peek system has high tool wear in the form of abrasion and adhesion [19]. Drilling comparison between brad spur drill, twist drill, and dagger drill showed better performance of brad spur drill [20]. Literature [21] also reports a 3D interlaminar damage criterion to quantity burr, tearing, and delamination in CFRP drilling. Another study [22] revealed that diamond-coated drill outperformed TiAlN-coated drill under MQL condition.

Davim and Reis [23] investigated the damage free drilling of CFRP using Taguchi and analysis of variance (ANOVA). The study revealed that out of different cutting parameters, cutting speed has the highest influence. Davim et al. [24] introduced a method to measure the adjusted delamination factor using digital analysis. The study revealed that digital method provided satisfactory results. Abra~o et al. [25] investigated the influence of cutting tool geometry for drilling of GFRP. It has been revealed that thrust force and delamination were not related directly, as the tool with highest thrust force provided lowest delamination area. It was also found that delamination was majorly influenced by the feed rate. Gaitonde et al. [26] investigated the high-speed drilling of CFRP by varying feed rate, cutting speed, and point angle. Response surface methodology (RSM) was employed to study delamination with respect to various process parameters. The study revealed positive influence of low feed rate and point angle on

decreasing delamination. The study also points out at the potential of lowering delamination using higher cutting speed. Rubio et al. [27] explored potential of high-speed machining (HSM) for the drilling of GFRP to lower the delamination. The study employed digital methodology for comparing conventional and adjusted delamination factors. Davim et al. [28] also investigated the drilling performance of hand layup GFRP using different process parameters. The study revealed that cutting velocity has the highest influence on the damage control of GFRP during drilling.

Delamination-based damage during the drilling operation is termed as main limiting factor towards the performance of drilling operation. Delamination is the parting of composite piles and categorized by the formation of interlaminar cracks in the CFRP material. It is common to observe two types of delamination during the CFRP drilling one at the entrance (peel-up delamination) and other at the exit (push-down delamination) of the drilled hole as shown in the Fig. 1b. Peel-up delamination forms due to the cutting force directing the cut material upward through the flute. Push-down delamination forms due to the bending caused by thrust force on the laminas just before exit [13]. Literature [14] also reports about the favorable and unfavorable force directions that are to reduce the delamination damage during the drilling operation. Figure 1c represents the schematic influence of cutting-edge roundness with respect to the feed rate involved. Cutting force ( $F_c$ ) is in the direction of the cutting velocity, whereas passive force ( $F_p$ ) involves all force components that are trying to push away the tool from the cutting interface. The resultant force ( $F_r$ ) describes the resultant of both  $F_c$  and  $F_p$ . As per the literature [14], increase in the edge roundness results in the increase in resultant force ( $F_r$ ) and passive force ( $F_p$ ). Schulze et al. [14] utilized the influence of edge roundness to reveal the attributes of drilling under the influence of tool wear that is very similar to the increase in edge roundness.

It is found in the metal cutting literature that inclined drilling process is rarely studied in academia, but it is being practiced in the aerospace and automotive sectors. The presented paper aims to characterize the interrelationships between hole inclination, lubrication/cooling methods, tool coating, and drill geometry with inclined hole bore surface quality and integrity during drilling of CFRP laminates. By considering the shear strength of the CFRP laminate used in this study, it does not seem like tool wear and its effect on the surface integrity would be a big problem for the current work. So, machinability assessment was evaluated by examining thrust forces, surface integrity using 3D confocal surface microscopy, and entry and exit delaminations of hole using scanning electron microscopy. The study will open new application areas for products related to the aerospace sector.

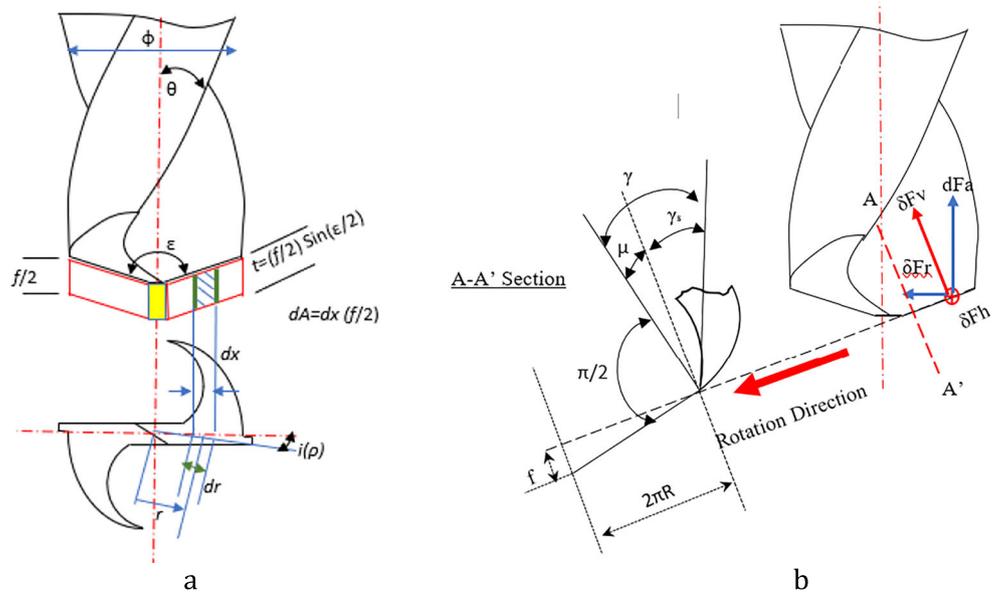
## 2 Chip load assessment in conventional and inclined drilling

As available in the classical metal cutting literature [29, 30], in a bi-dimensional machining system, cutting forces are directly associated with the chip area or chip load. Drilling operation is very complex in terms of cutting and chip load assessment. Cutting with drill bit is composed of three different regions based on chisel edge and cutting lip cutting modes. The cutting mode with chisel edge is further sub-divided into indentation zone in the middle of the drill bit and orthogonal cutting at chisel edge away from the center. In the indentation zone, material does not cut but extrude only with plastic deformation [29]. Outside the indentation zone, cutting is performed under orthogonal cutting mode with negative cutting angle. However, the cutting action at the cutting lip is analyzed using three-dimensional oblique cutting formulation. As a radial distance increases at the cutting lip, the parameters such as cutting velocity, back rake angle, side rake angle, and normal rake angle also differ. To solve this issue, a normalized radial coordinate ( $\rho = r/R$ ) is utilized, where ( $r$ ) is the radial distance on the cutting lip and distance ( $R$ ) is the drill radius. So, there is a need to divide the cutting lip into small elements and then solve the elemental forces relation using integration. The associated formulation is discussed in detail in the available literature [29, 31–33]. It has been observed that cutting process is efficient towards the outer part of the cutting lip due to higher rake angle and cutting velocity, whereas cutting action is more dominated in the middle of the drill due to low cutting velocity and rake angle (negative in chisel edge), where  $i(\rho)$  is the inclination angle and can be represented using Eq. 1.

$$i(\rho) = \sin^{-1} \left[ \frac{w}{\rho R} \sin \left( \frac{\varepsilon}{2} \right) \right] \quad (1)$$

Literature [34] classifies chip formation in fiber reinforced plastics as four different types (type I, type II, type III, and type IV) (Fig. 2). Figure 3 represents these chip types by showing different fiber orientation angles ( $0^\circ$ ,  $45^\circ$ ,  $90^\circ$ , and  $135^\circ$ ) with respect to the drill bit rotation. As the drill bit rotates, the fiber orientation of CFRP also varies in between  $0^\circ$  and  $180^\circ$ . The type of cutting operation and chip formation varies significantly as the fiber orientation angle orientation changes. It can be observed that at fiber orientation of  $0^\circ$ , fibers are easy to delaminate as compared with other orientations. It will result in type I chip formation, and delamination is termed as fiber-matrix debonding [34]. When fiber orientation angle is between  $15^\circ$  and  $75^\circ$ , fibers are fractured due to the compressive shear caused by the cutting edge. At the fiber orientation angle in between  $75^\circ$  and  $90^\circ$ , the cutting involves fracture due to compression, and type III chips are formed. For fiber orientation angle  $90^\circ$  and beyond, the cutting process

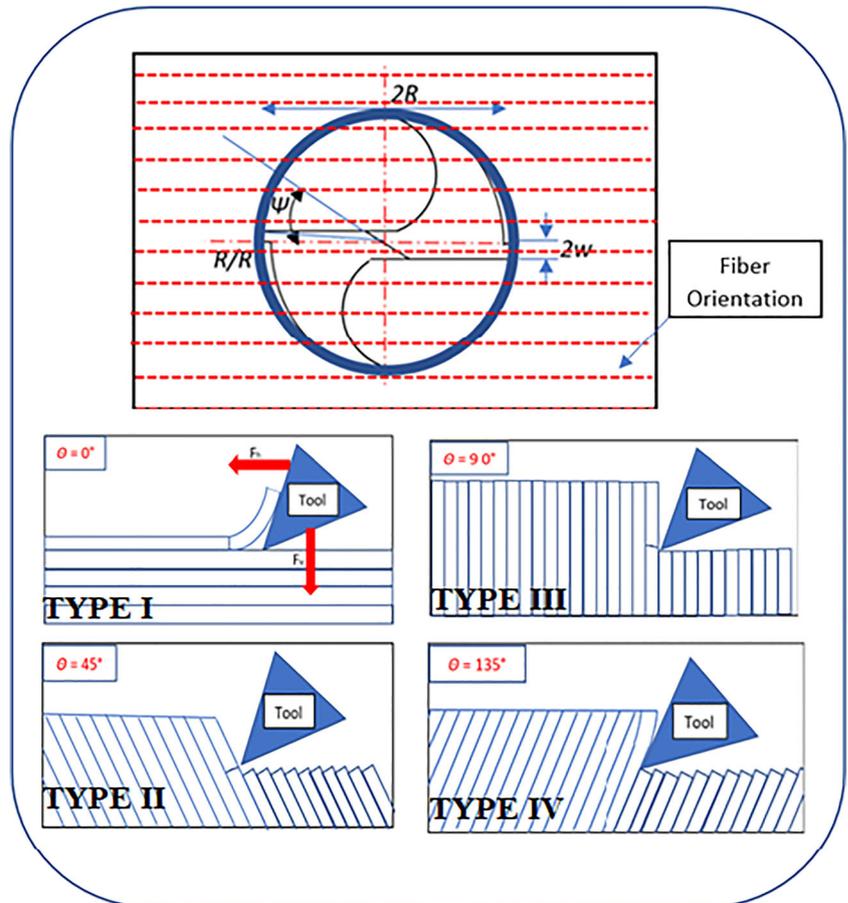
**Fig. 2** **a** Chip load present on the element at cutting lip. **b** Representation of cutting forces at the cutting lip with geometric parameters such as rake angle [32]



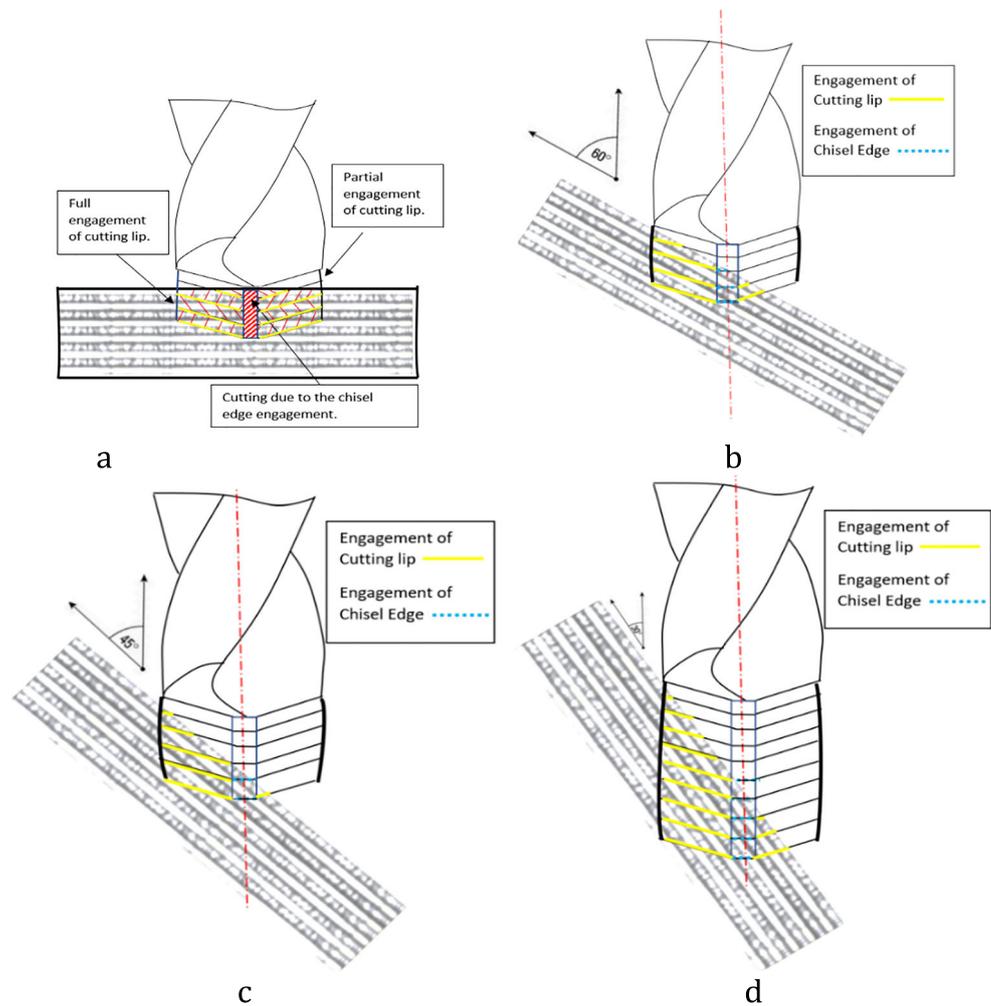
results in intermittent fracture along fiber axis. It can be observed that more fiber pull-outs are experienced in this case [34].

Figure 4 represents the interaction of cutting lips and chisel edge with the CFRP laminates at the entry of the hole under different inclination angles of 30°, 45°, 60°, and 90°. It can be

**Fig. 3** Top view representing drill bit cutting lip interaction with fiber orientation



**Fig. 4** Schematic illustration of chip load in drilling using chisel edge and cutting lip engagement. **a** 90° inclination. **b** 60° inclination. **c** 45° inclination. **d** 30° inclination



observed that inclination angle of 30° is showing the interaction of cutting lip with the CFRP laminates instead of chisel edge indenting and cutting the laminate. This means that the hole entry at angle 30°, 45°, and 60° are more challenging as compared with 90° angle. There is also a chance of slippage at lower inclination angles. This was validated through the thrust force signatures as well.

### 3 Experimental method and design

#### 3.1 Experimental setup

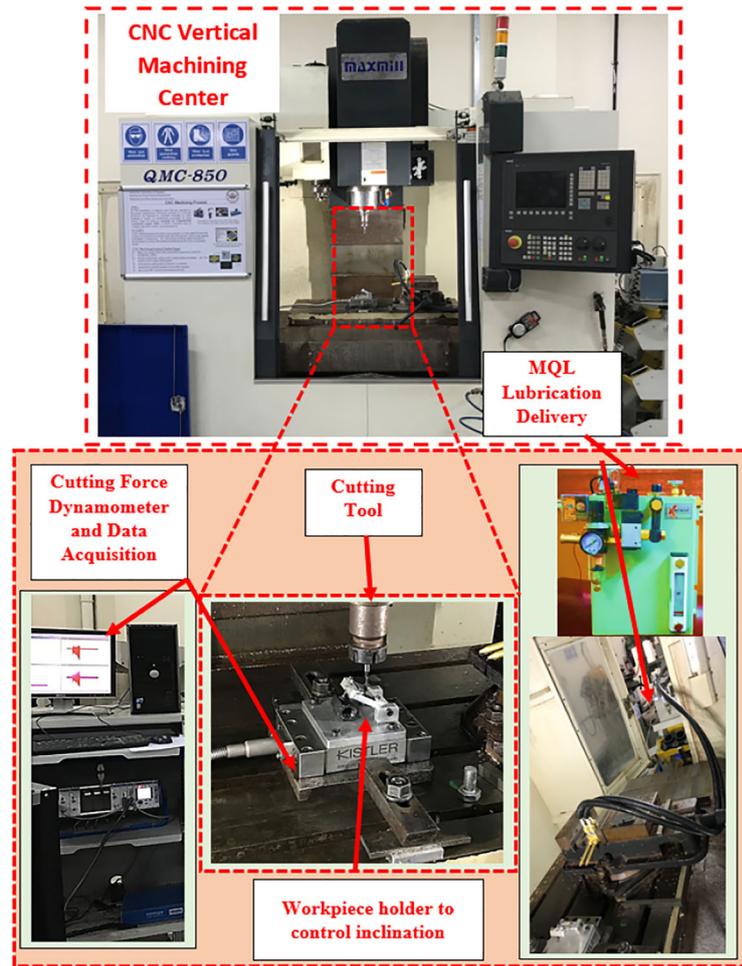
The drilling experiments on CFRP material were conducted using vertical machining center (Model QMC– 850, Maxmill Machinery, Taichung City, Taiwan). The technological specification of Maxmill VMC-vertical machining center is presented in appendix A. To evaluate the drilling performance, cutting forces, and quality of the drilled inclined holes were monitored in this study. When it comes to the drilling operation, cutting forces can provide useful information about the

overall cutting process. However, the hole quality provides useful feedback towards the service life of the product. The cutting forces were captured using multi-channel dynamometer (Model 9129AA, Kistler Instrument Corp, MI, USA) with charge amplifier (Model 5070, Kistler Instrument Corp, MI, USA). Technical specifications are mentioned in appendix A. To drill holes at specific inclination angle, special fixture was developed to conduct this study. Figure 5a and b represents the schematic illustration of the drilling experimentation. To analyze the drilled hole quality, scanning electron microscope (Model VEGA 3, Tescan, Czech Republic) and confocal were utilized.

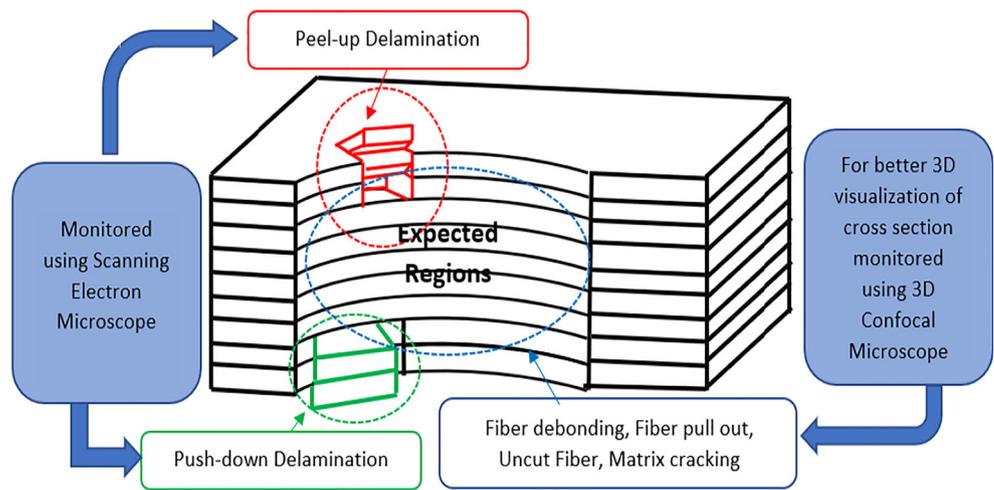
#### 3.2 Cutting tool and workpiece details

The study utilized two different material grades of drill bits, namely, KC 7315 and KC7325. Cutting tools were selected as advised by the manufacturer (both grades were classified under solid carbide drill with similar diameter and other geometric features but with different coatings material). Grade KC 7315 is a multilayer TiAlN-PVD coated with better tool life at

**Fig. 5** **a** Experimental setup schematic illustration. **b** Surface integrity investigation schematic illustration



**a**



**b**

**Table 1** Technical specifications of drill bits

Tool 1	Tool 1	Tool 2
Drill material grade: B966A03000 KC7315		Drill material grade: B051A03000CPG KC7325
Grade	KC7315 is a fine-grain carbide with a TiAlN-based PVD multilayer coating	KC7325 grade contains a double coating for broad-band applications, and a TiN top layer serves as a wear indicator
<u>Geometric dimensions:</u>	3 mm	3 mm
Drill diameter		
Total length	62 mm	62 mm
Flute length	20 mm	20 mm
Maximum drill depth	14 mm	14 mm
Length shank	36 mm	36 mm
Drill point length	0.5 mm	0.5 mm
Shank dia	6 mm	6 mm
Point angle		140°

higher cutting speeds, whereas KC 7325 grade is double-coated drill, and a TiN coating at top layer facilitates wear indication. Both drills were provided and recommended by the Kennametal. Table 1 represents the drill geometry and related information.

The workpiece consisted of 10 different layers of alternate 45° and 0° configurations. The workpiece behavior was quasi-isotropic in nature. Figure 6 shows the CFRP layer structure at the cross section. Table 2 has information about the other CFRP preparation settings such as type of resin used and fiber matrix fraction.

### 3.3 Design of experiments (DOE)

Design of experiment was created by varying cutting parameter under different cooling/lubrication strategies. Selection of

spindle speed and feed rate was performed carefully as advised by the cutting tool manufacturer for the drilling of CFRP material. The study also explored the drilling performance of CFRP at different inclination angles (30°, 45°, 60°, and 90°). The lubrication under compressed air was carried out at pressure of 3 bar. Table 3 shows cutting conditions utilized in this work.

### 3.4 Green lubricant and MQL information

To drill holes in the CFRP material under MQL setup, a green lubricant (Ultracut GF060711) was employed in the experimentation. The KENCO MQL setup consisted of two nozzle delivery system. The green lubricant contained fatty alcohols as the main ingredient and has biodegradable, non-toxic, odor-

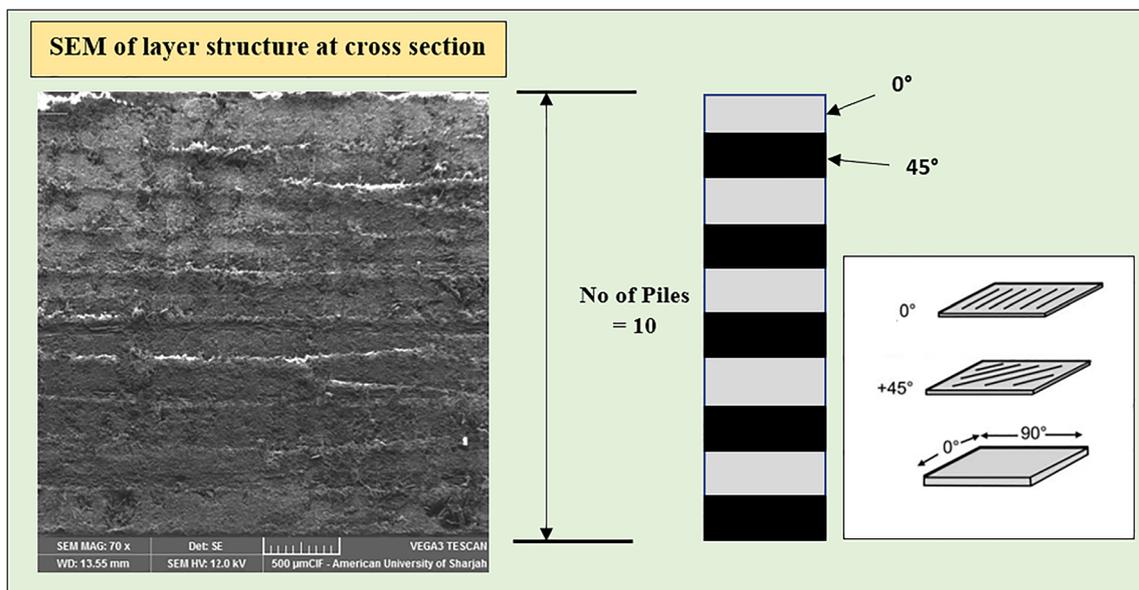


**Fig. 6** SEM micrograph of the cross-section of CFRP layer structure

**Table 2** Technical specification of CFRP material

CFRP information	Details
Layer orientation	0° and 45°
No. of plies	10
Manufacturing step	Autoclave cured
Resin type/grade	Aerospace grade toughened epoxy matrix
Carbon reinforcement type/grade/Vol%	High-strength carbon fibers, Vf~52%. All ply architecture is the same as ones on the surface
Curing and post-curing in auto calve	Cured at 180 °C

free, and non-water polluting behavior. Table 4 shows properties of green lubricant.

## 4 Results and discussion

In this section, the results have been discussed by considering the thrust force component, surface integrity, and examination of the drilled hole quality. To evaluate the hole quality, special attention has been given to the entry and exit conditions, burr formation, and delamination with the help of scanning electron microscope. 3D surface profilometer was utilized to analyze the surface integrity and capture the fiber and matrix fracture mechanisms. Scanning electron microscopy was performed in order to evaluate the hole quality machined at different inclination angles. SEM helped to observe the hole delamination. Delamination is considered to be a damage that occurs in between different laminates of the CFRP material and mainly controlled by the interlaminar fracture toughness and modulus of elasticity.

Thrust force has been attributed as one of the most important machinability indicators when drilling CFRP composite material. Thrust force directly affects the drilled hole's integrity and has a controlling influence towards the drilling-induced delamination (Fig. 7) [35].

**Table 3** Cutting parameters utilized for drilling CFRP

Parameters	Levels
Cutting Speed (m/min)	25, 35, and 45
Feed rate (mm/min)	250, 500, and 750
Tool materials	KC7315 KC7325
Lubrication methods	Dry Compressed air Minimum quantity lubrication (MQL) Conventional flood
CFRP hole inclination	30°, 45°, 60°, and 90°

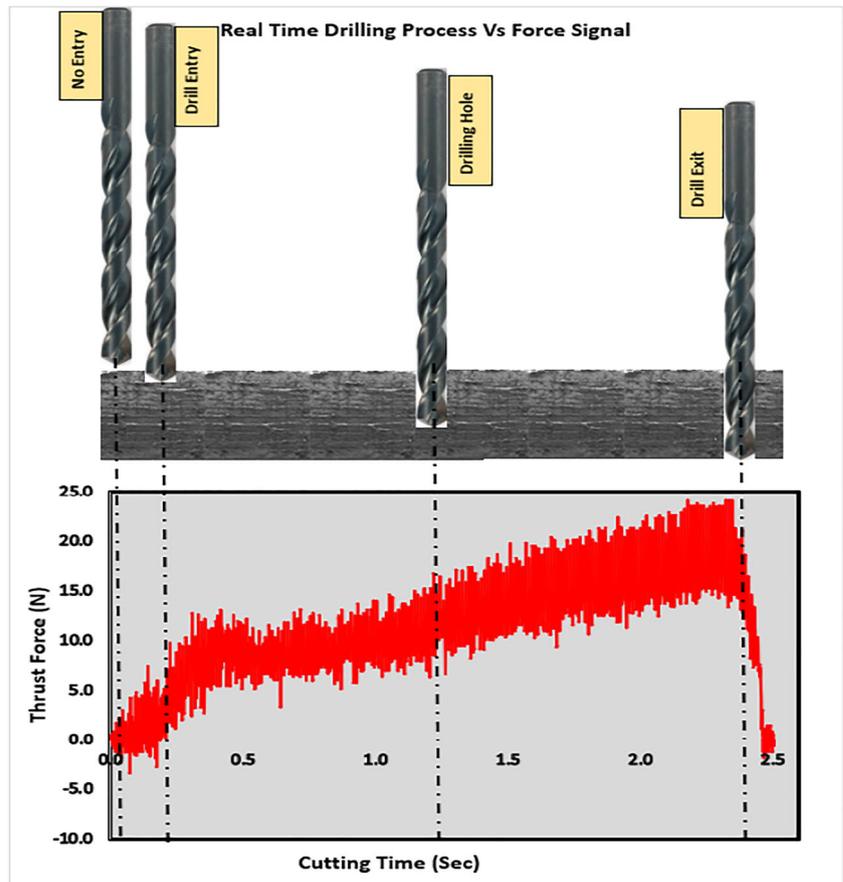
It has been reported in the literature [36] that thrust force is linked with the delamination, and below the critical level of thrust force no delamination occurs. Interaction of the cutting tool and workpiece material was captured by monitoring the cutting forces. It has been observed that thrust force gradually increases from drill entry till drill exit. In order to understand the fracture of CFRP composites, it is important to understand the mechanisms of crack propagation in the CFRP composites. Literature [37] points out three basic modes of fracture in the CFRP composites. Fracture mode I results in the opening of laminates mainly due to the application of tensile stress. Fracture mode II results in the shearing or sliding of laminates when loaded under shear stress acting parallel to the crack plane as shown in Fig. 8. Fracture mode III results in the tearing of laminates due to the application of shear stress acting parallel to the crack plane as shown in Fig. 8.

In the case of CFRP material, the mentioned three common fracture modes can generate a number of CFRP-specific failure modes due to the presence of fibers, matrix, and fiber-matrix interface. These CFRP-specific failure modes include matrix cracking, matrix deformation, fiber fracture, fiber debonding, interlaminar delamination, and fiber pullout. Some of these defects are shown in Fig. 9. The chip formation and cutting mechanism in conventional metals and their alloys are linked with the shearing and associated plastic deformation. Because of the inhomogeneity and anisotropic behavior of the CFRP material, the interaction of cutting edge in drilling and CFRP laminates is very complex at the cutting interface.

**Table 4** Specifications of green lubricant (Ultracut GF060711)

Parameters	Values
Density at 15 °C	0.84 g/ml
Kinematic viscosity at 20 °C	51 mm <sup>2</sup> /s
Flash point	150 C°
Copper corrosion	1-100A3 Degree
Pour point	-58 C°

**Fig. 7** Thrust force time signal with respect to the progress of drilling process



Sreejith et al. [39] mentioned that in FRPs, the cutting mechanism and chips are formed due to plowing, cutting, and cracking. Plowing was attributed as deformation, cutting was taken as shearing, and cracking was due to fracture, delamination, and buckling [40].

Fiber orientation has been attributed as one of the most significant factors towards the cutting mechanics, chip

formation, and surface integrity when machining CFRP. In addition to this, the orientation of fiber with respect to the cutting edge is continuously changing for one complete revolution of the drill rotation. Keeping in view the cutting mechanics involved in drilling operation, literature [42] explains that chisel edge enters into the first ply, and then main cutting edge performs the cutting action in downward and as well as

**Fig. 8** Different types of fracture modes to facilitate crack propagation in CFRP

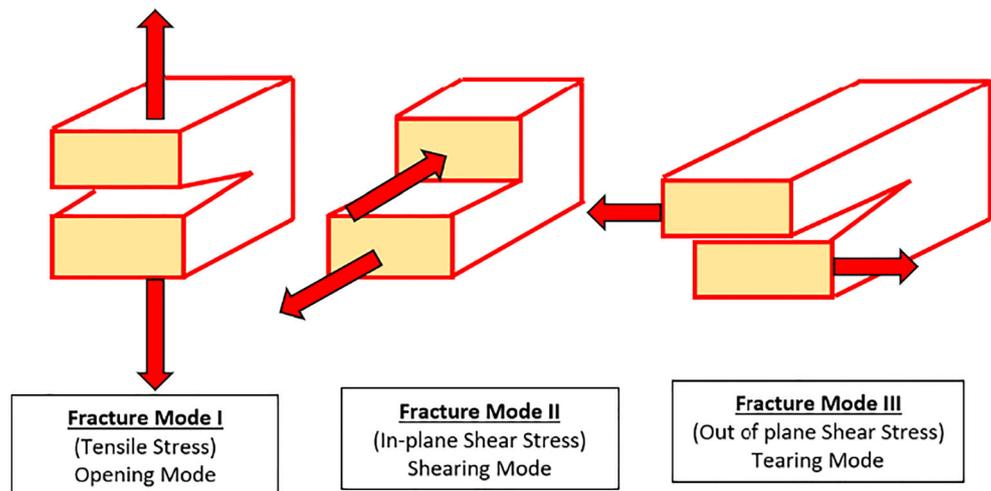
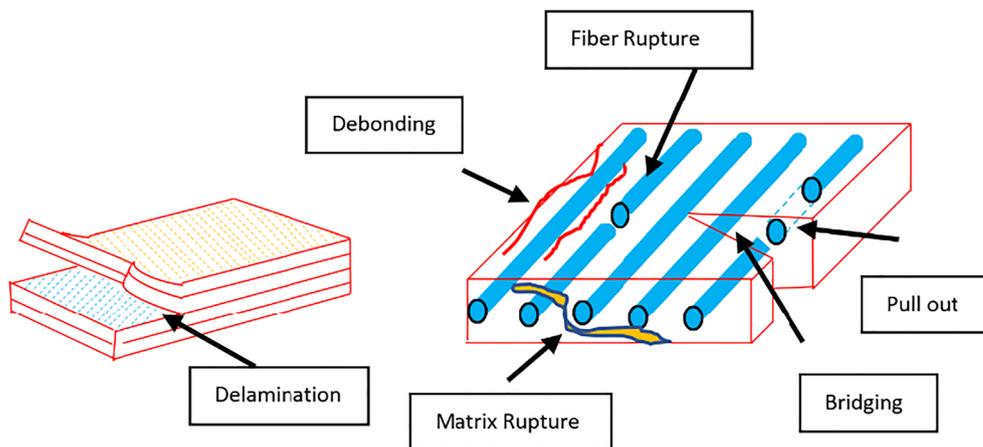


**Fig. 9** Common failure modes of CFRP composites (adopted from [38])



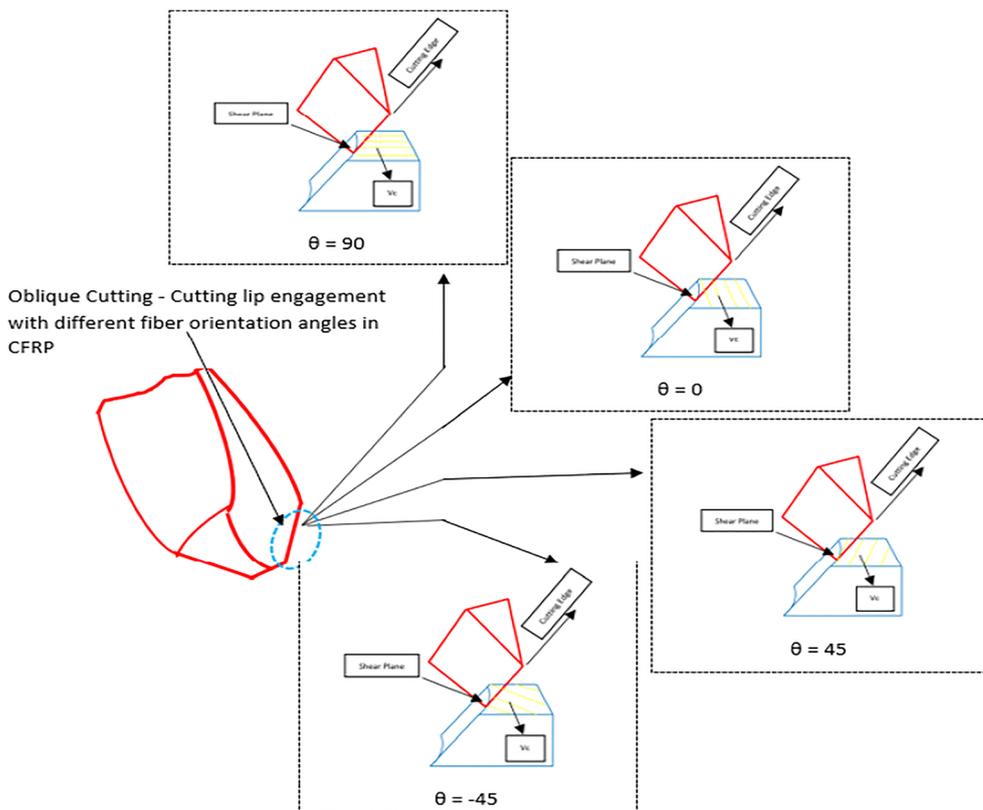
in the peripheral direction to cut the uncut CFRP. Because of less support on the exit side, main cutting edge tends to bend and tear away the fibers on outer side. For CFRP drilling, the cutting mechanisms are very complex due to interaction of main cutting edge with the laminated plies under different fiber orientation. Figure 10 shows the fiber orientation and cutting velocity direction for the main cutting edge. It has been observed that the cutting performance was affected due to more intense fiber-tool interaction for the configuration of  $-45^\circ$  and also provided higher delamination. It is because

the feed force can exceed the limit for fiber-matrix cohesion [41]. The associated chip formation types (type I, type II, type III, and type IV) with fracture modes are discussed already in previous sections.

**4.1 Effect of inclination**

The effect of inclination angle was also investigated by observing the thrust forces as shown in Fig. 11b, c, d, and e. In order to reflect chip load and engagement of chisel edge and

**Fig. 10** Fiber orientation interaction with the main cutting edge under CFRP drilling (adopted from [41])



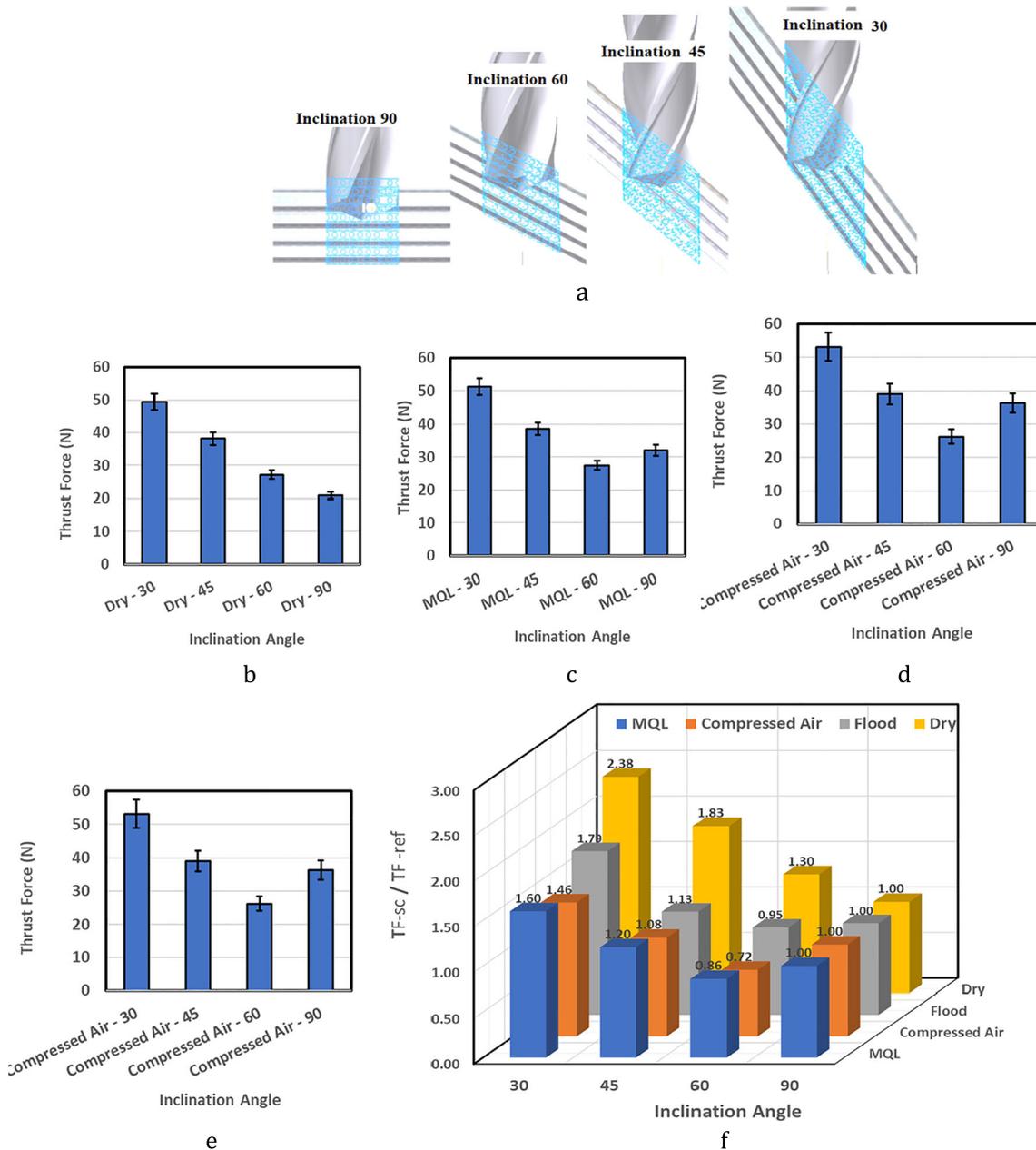


**Fig. 11** a Chip load reflection under different inclinations. b Thrust forces at various inclination angle using KC7315 grade at cutting speed of 45 m/min and feed rate of 250 m/min—dry cutting. c MQL. d Compressed air. e Flood. f All thrust forces showing the relative effect with reference to 90°

cutting lip, Fig. 11a is constructed using CAD modeling. When inclination changed from 90° to 30°, higher thrust forces were observed. As illustrated earlier in the schematic diagrams, 30° inclination angle involved more workpiece material engagement among other inclinations; as a result the cutting action in this case is more difficult and provided higher magnitudes of the thrust forces. A possible reason of this can be linked to the interaction of drill's chisel edge and cutting lips with the CFRP laminates at the hole entry. In inclined drilling, the hole initiation did not start from the chisel edge.

However, it is observed that cutting lip that is towards the surface of the workpiece material enters first in the CFRP laminate. As shown in Fig. 11f, in dry cutting thrust, forces were found 2.38 times higher in the 30° inclination when compared with the reference 90° conventional inclination angle. For 30° inclination, compressed air provided lowest increase (1.46 times) in the thrust forces.

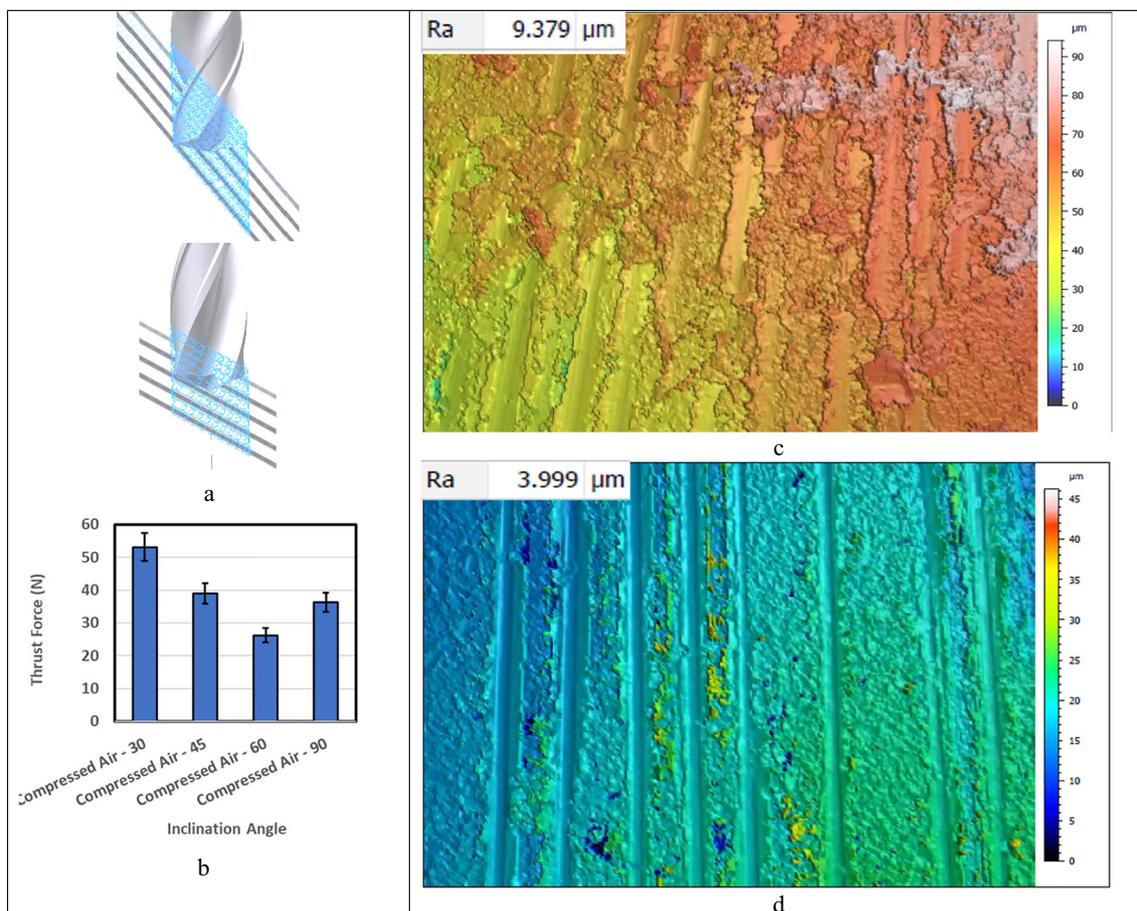
The type of failure modes during the CFRP drilling depends on the cutting direction and fiber orientation. Most commonly reported fracture modes in literature are fiber

tensile failure, matrix tensile failure, fiber compression failure, and matrix compression failure [43, 44]. The failure modes occur in combination and generate different forms of chips with particular surface integrity. Literature also reports different chip formation modes as fiber buckling, fiber cutting, fiber delamination, fiber deformation, fiber shearing, and fiber pull-out [44, 45]. In the current study, the following modes such as (1) tensile fracture, (2) in-plane shear, and (3) out of plane shear/delamination have been witnessed under 3D surface roughness analysis.

Figure 12a represents the interaction of drill with CFRP laminates at different inclination angles. It can be observed that interaction of drill cutting edge and CFRP laminates experiences more elastically recovered broken fibers in 30° inclination angle. At this inclination, it was difficult for drill cutting edge to penetrate initially. High value of thrust force associated with the 30° inclination is linked with the higher chip load during this inclination as compared with the 60° as shown in Fig. 12b. Figure 12c and d shows the surface roughness condition at both

inclination angles. Figure 12c represents the surface roughness to be high (9.379  $\mu\text{m}$ ) at 30° inclination as compared with the surface roughness of 3.999  $\mu\text{m}$  at 60° inclination. In both Fig. 12c and d, the presence of tool marks is also visible. It is understood that inclination of workpiece material during drilling operation can generate uneven distribution of the thrust force and torque resulting in more complex drilling-induced damage and delamination. At an angle of 30°, the uneven distribution of thrust force and torque is maximum as half of the cutting lip is engaged initially, and other cutting lip is in the air.

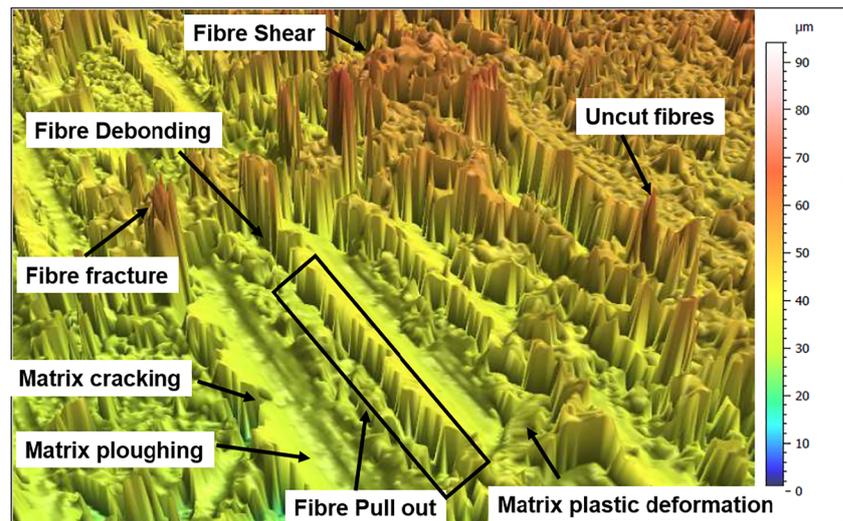
Figure 13 represents the 3D confocal surface analysis of CFRP drilling at 60° inclination under compressed air-cooling method. As pointed out in Fig. 13, several failure mechanisms have been observed. These mechanisms consist of fiber shearing, fiber debonding, fiber tensile fracture, uncut fiber, matrix cracking, matrix plastic deformation, and fiber pull out. In the current study following modes such as (1) tensile fracture, (2) in-plane shear, and (3) out of plane delamination have been



**Fig. 12** a Interaction of drill geometry with the CFRP laminates at different inclination angles. b Thrust forces for the inclination angles for compressed air cooling. c 3D surface roughness of CFRP when

drilling at 30° using 7315 tool at 45 m/min and 0.05 mm/rev under compressed air. d 3D surface roughness of CFRP when drilling at 60° using 7315 tool at 45 m/min and 0.05 mm/rev under compressed air

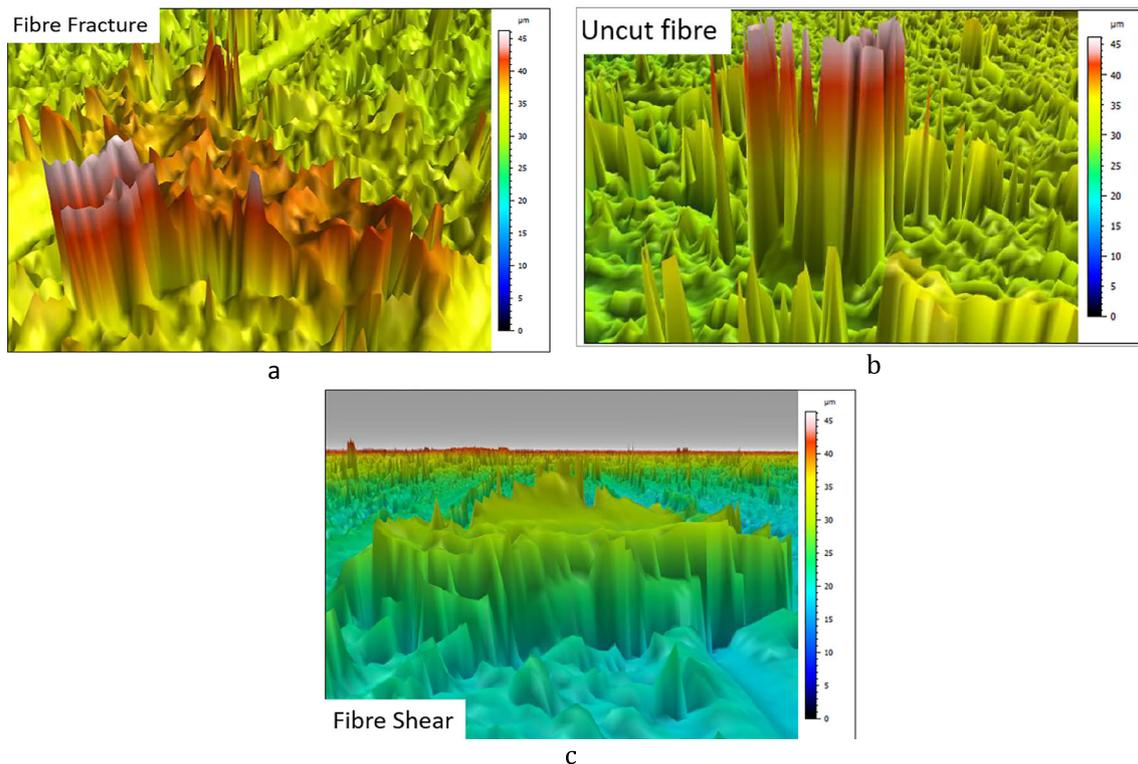
**Fig. 13** 3D Surface roughness of CFRP when drilling at 60° inclination using 7315 tool at 45 m/min and 0.05 mm/rev under compressed air



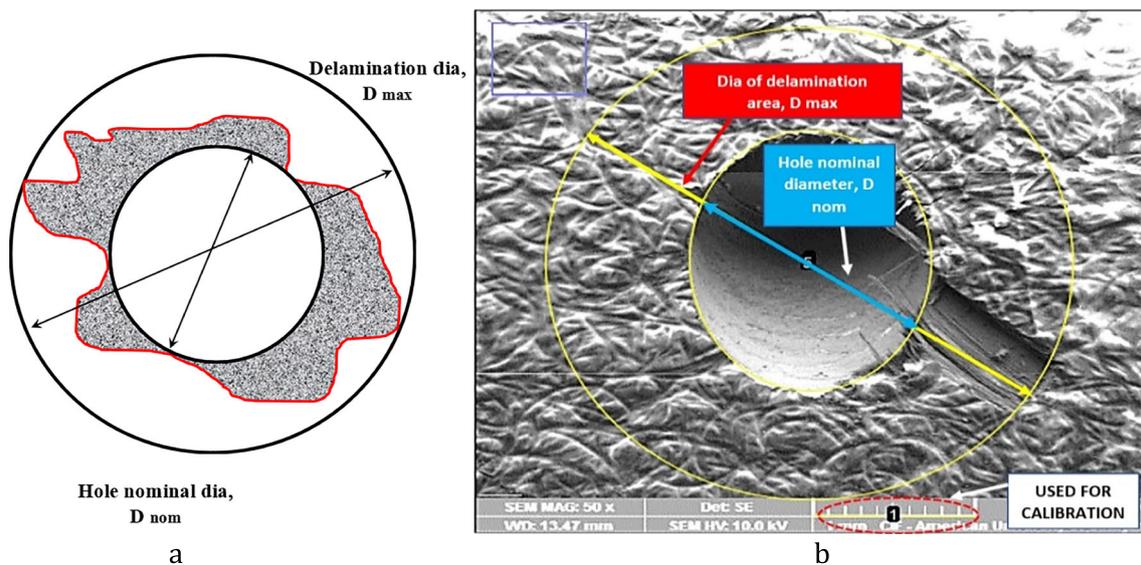
witnessed under 3D surface roughness analysis. In Fig. 14a, fiber fracture can be observed, and it would be a result of mode 1, tensile fracture, and mode 3, out of plane delamination. In Fig. 18b, the presence of uncut fiber is visible, and it is due to mode 1, tensile fracture, and extent observed here was more significant than the one observed in previous Fig. 14a. In Fig. 14c, fiber shear can be observed clearly, and it is the result of mode 2, in-plane shear.

Figure 15a and b represents the schematic illustration of delamination factor ( $F_D$ ) using maximum delamination diameter ( $D_{max}$ ) and hole nominal diameter ( $D_{nom}$ ) to quantitatively represent pull out delamination. Delamination factor is widely used in the literature to quantify pull out delamination as shown in Eq. (2) [46].

$$F_D = D_{max}/D_{nom} \quad (2)$$



**Fig. 14** 3D Surface roughness of CFRP using 7315 tool at 45 m/min and 0.05 mm/rev under compressed air (a). Fiber fracture at 30°. (b) Uncut fiber at 30°. (c) Fiber shear at 30°



**Fig. 15** **a** Schematic illustration of delamination factor ( $F_d$ ). **b** Sample calculation for the assessment of push out delamination factor ( $F_d$ )

In Fig. 16, comparison of dry cutting with MQL was presented for  $45^\circ$  inclination, and chilled air was compared with the MQL for  $30^\circ$  inclination angle. The condition of dry cutting at entry has more delamination than MQL at  $45^\circ$  inclination angle. Similarly, the chilled air provided more delamination than MQL at entry for  $30^\circ$  inclination angle. For MQL both inclination angles provided very severe fiber pull-out with the presence of uncut fibers at exit conditions as shown in Fig. 16d. However, highest pull out delamination was observed for dry cutting. Similarly, in Fig. 17, other SEMs of different conditions have been reported as it was not possible to provide SEM of each condition. For  $30^\circ$  inclination angle, MQL and flood cooling methods have been compared, and it has been observed that less delamination was observed in MQL at the entry condition. The SEM revealed that at  $30^\circ$  inclination angle, both cooling methods have severe fiber pull-out and the presence of uncut fiber at the exit condition. MQL and flood cooling methods were again compared for  $90^\circ$  inclination angle, and it was observed that MQL provided better results for delamination as compared with the flood cooling as shown in Fig. 17b. It has been observed as a generic trend that for inclined hole drilling, both MQL and flood cooling environments provided very severe delamination (fiber pull-out and uncut fibers) at the exit conditions. This behavior can be linked with the presence of weak interlaminar bonding coupled with higher thrust forces.

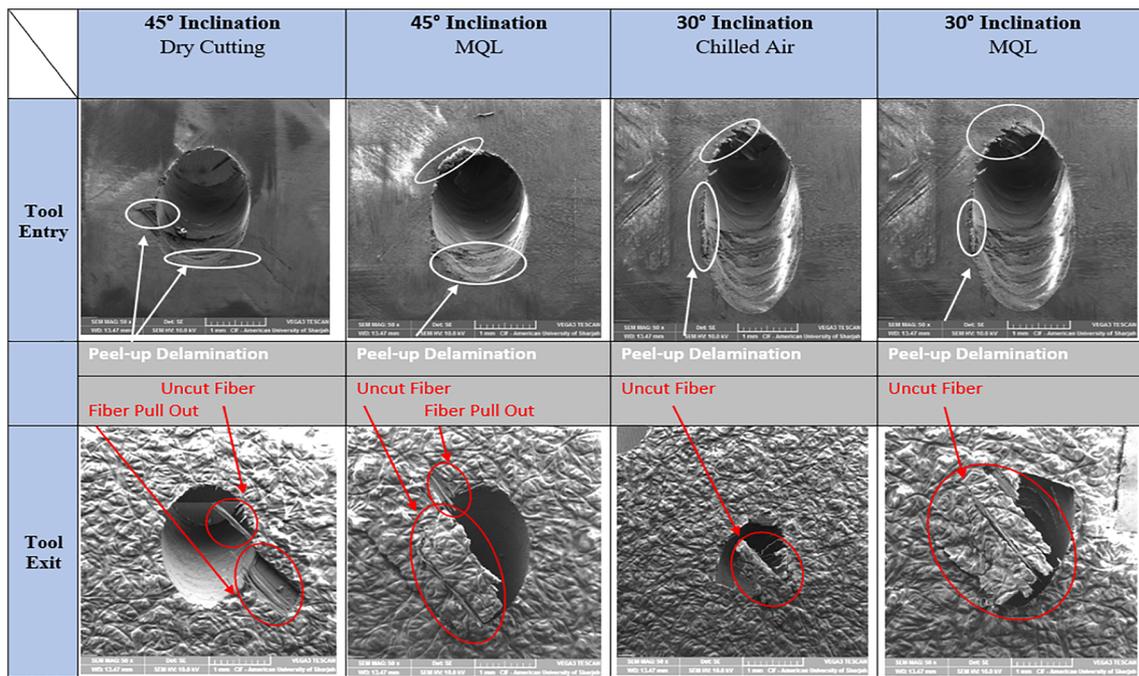
#### 4.2 Effect of lubrication methods

To have comparison of different cooling and lubrication methods, average force value from drill entry till exit has been evaluated. The average values of thrust force under different

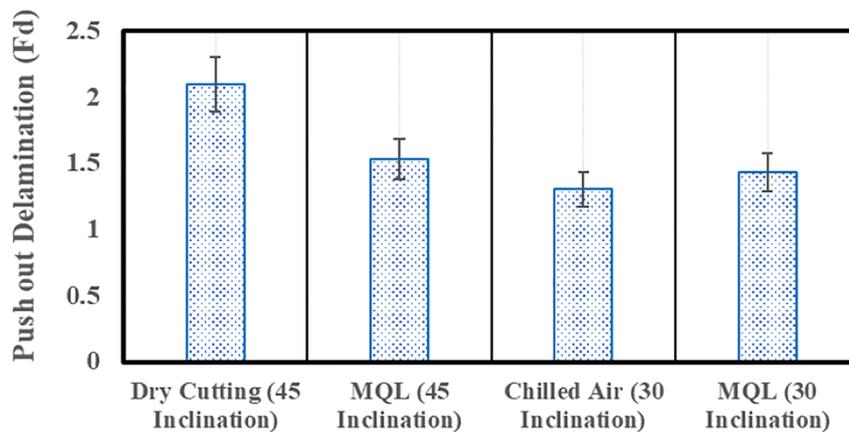
lubrication methods have been reported in Fig. 18. It is observed that there was minor difference in the cutting forces for different lubrication methods. The CFRP plate was of only 3-mm thick; as a result the thrust force was low in magnitude in all cases.

The generic trend represents that dry cutting provided the lowest force at inclination of  $30^\circ$  and  $90^\circ$ . A possible explanation of this behavior can be linked with the heat accumulation when drilling CFRP under dry cutting mode. CFRP material has generally low thermal conductivity and low heat capacity; as a result heat can be easily generated and accumulate in the cutting zone [47]. Literature [48] points out that glass transition temperature of CFRP is around  $160\text{--}200^\circ\text{C}$ . The formation of high cutting temperature during dry cutting softens the resin matrix [49]. Many studies showed that the soften matrix decreases roughness due to matrix smearing [50]. The higher values in the thrust force represent that effective cooling took care of cutting temperature and the resin matrix was still intact. For inclination of  $30^\circ$ , the drilling produced highest thrust forces for all lubrication methods.

Noticeable fluctuations in the thrust forces were observed at inclination of  $90^\circ$ . Figure 19 represents the 3D confocal surface analysis conditions observed at  $90^\circ$  inclination for different lubrication methods. It can be observed that dry cutting provided the maximum value of surface finish  $7.950\ \mu\text{m}$ . It can be observed in Fig. 19a that matrix plastic deformation is visible as compared with the flood cooling in Fig. 19d. This clearly points out the presence of high cutting temperature that softened the temperature matrix. In addition, uncut fiber lengths are also visible in Fig. 19a pointing out the fracture mode I. In Fig. 19d, the CFRP surface looked more like a brittle fracture under fracture mode II. The fiber debonding and uncut fiber lengths are clearly visible under flood cooling



a

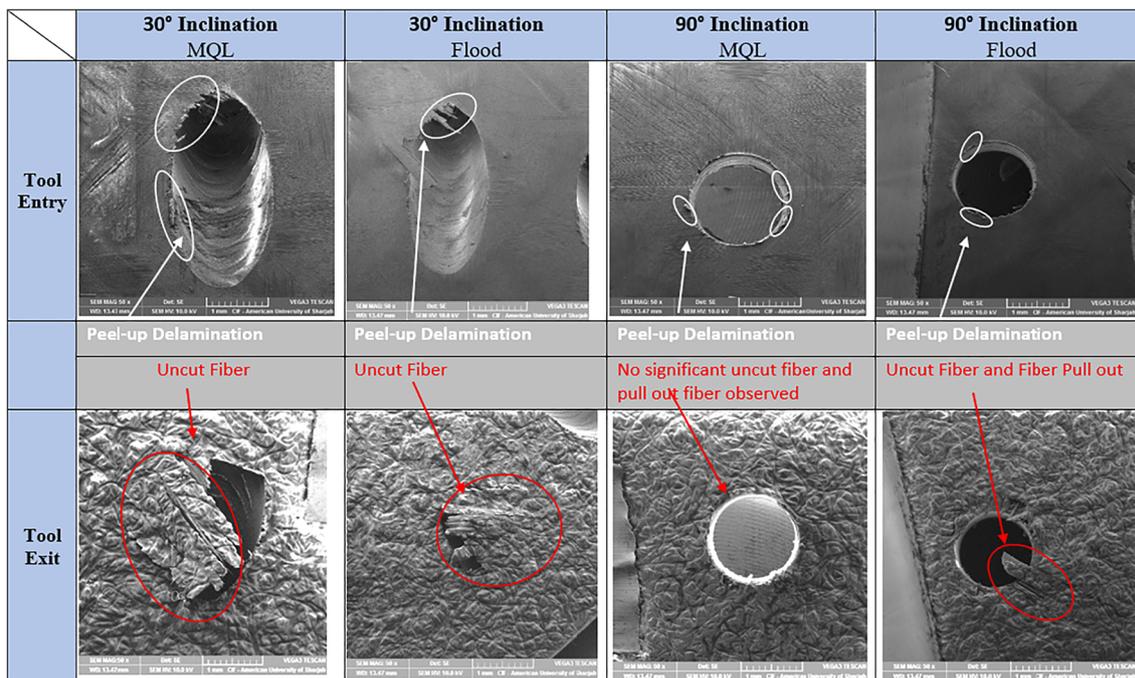


b

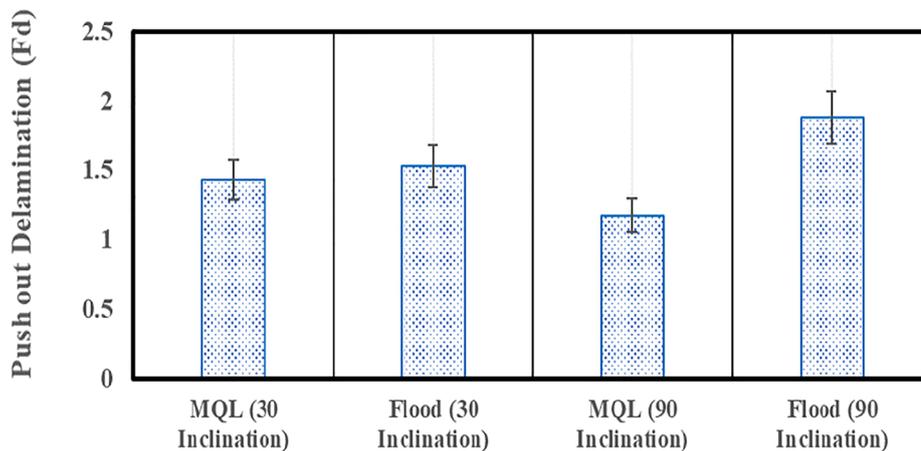
**Fig. 16** a KC 7315 grade cutting tool for entry and exit profiles when drilled at inclination angles and lubrication/cooling strategies. b Delamination factor calculated for push-out delamination at exit

pointing the fact that the fracture in this condition was too brittle with fracture mode I. Plowing track is also visible in Fig. 19d. The plowing track represents the fiber split and then debonding from matrix. These surface roughness conditions were found in agreement with the thrust forces. The surface roughness observed under MQL ( $3.797 \mu\text{m}$ ) and compressed air ( $4.457 \mu\text{m}$ ) was better than dry and flood cooling methods as shown in Fig. 19b and d. In both figures, uncut fiber lengths were observed majorly under fracture modes I and mode III. The extent of these fracture modes was much lesser in MQL and compressed air as compared with the dry and flood cooling methods. Fiber pull out is the inherent feature of

CFRP surface caused due to cutting mechanism and influenced by tool wear and cutting-edge rounding as shown in Fig. 19b and c. The extent of uncut fiber length was also less in the MQL as compared with the compressed air. It is due to useful lubrication influence that affects tool wear. Delamination happens in different laminates at the entry and exit of the CFRP material mainly known as peel-up and push-down mechanisms. Peel-up delamination is due to the initial penetration caused by the drill geometry and abrades the laminar material. As the drill geometry penetrates inside the laminar material, the abraded material moves up along the flute of the drill. The peel-up delamination is a function of drill



a



b

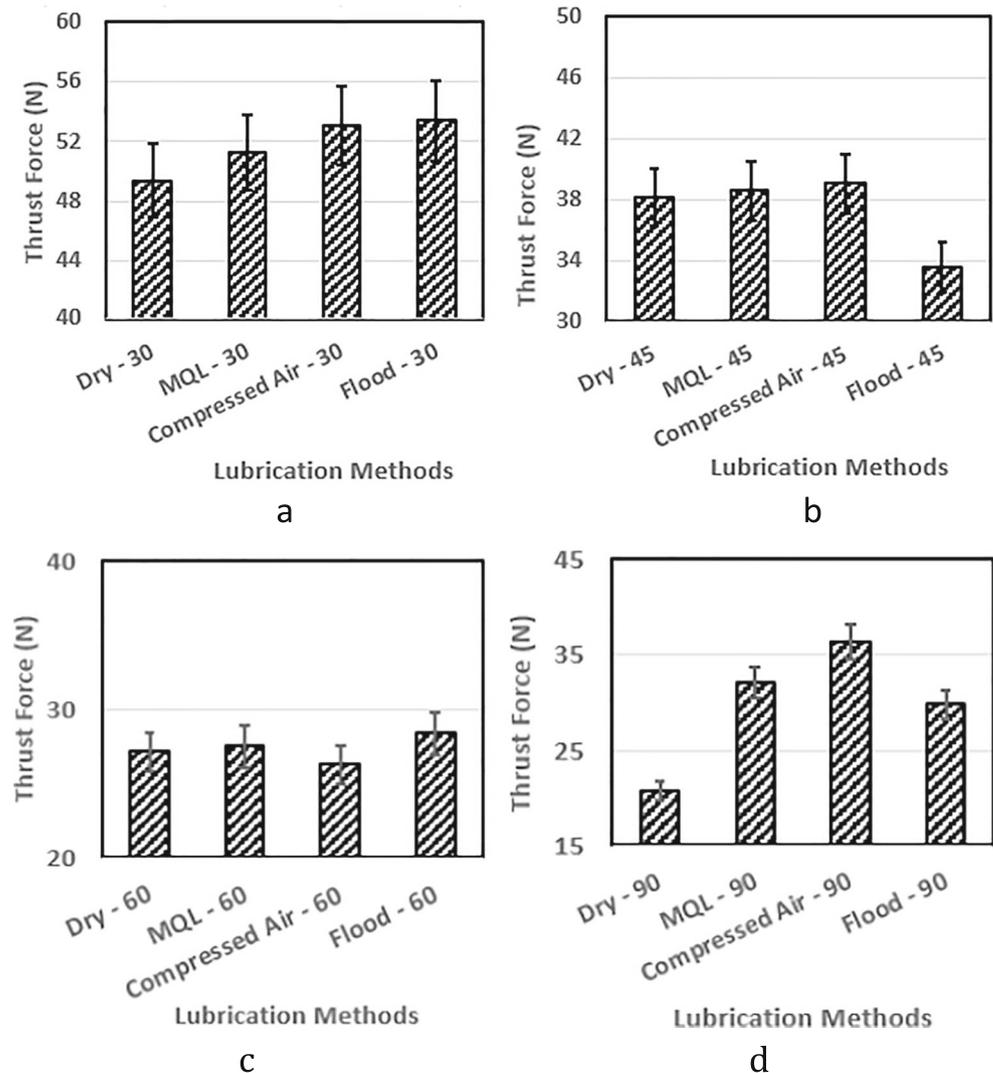
**Fig. 17** a KC 7315 grade cutting tool for entry and exit profiles when drilled at inclination angles and lubrication/cooling strategies. b Delamination factor calculated for push-out delamination at exit

geometry and friction at cutting interface. Push-down lamination is the result of high compressive load that chisel edge exerts on the laminates. Most of the times at exit, this load exceed the interlaminar bond strength of the material causing laminar delamination at exit. A well-studied thrust force behavior can significantly reduce these delamination mechanisms [51].

Figure 20 represents the hole entry and exit conditions for KC 7315 cutting tool grade when drilled at 60° inclination under different lubrication and cooling strategies. At tool exit push-down, delamination is shown for

different lubrication strategies. This sort of delamination is formed when crack form and proceed in between the two bonded laminates. Type I: Tensile opening fracture appears at the hole exit. Based on fiber orientation angle, push-down delamination appears significant for fibers at orientation beyond 90°. More or less very similar delamination was found at the entry condition for all types of lubrication strategies. At the hole exit conditions, compressed air provided the best outcome. Dry air provided very limited fiber pull-out; however MQL and flood provided severe fiber pull-out and the presence of uncut

**Fig. 18** Thrust forces for drilling CFRP using KC7315 grade cutting tool under different lubrication methods at cutting speed of 45 m/min and feed rate of 250 m/min



fibers at the exit conditions as shown in Fig. 20b. Fiber pull-out mechanism is linked with the weak interlaminar bonding. When drill thrust, force exceeds certain limit at the exit of hole and due to the absence of support for the bottom laminate, fiber pull-out occurs.

### 4.3 Effect of cutting tool material grade

The study incorporated two different types of drill materials, namely, KC7315 (fine-grain carbide with PVD-TiAlN) and KC7325 grade (double coated with TiN top layer). The thrust force plotted against both cutting tools showed that 7325 grade (TiN top coating) provided lower thrust forces as compared with the 7315 grades (with PVD TiAlN coating). Comparison has been presented for MQL lubrication only as similar trends were observed for other lubrication methods as well. Keeping in view that TiAlN coating is superior to TiN in terms of tool life

and ability to sustain high cutting temperature. The possible reason of this thrust force behavior is linked with the performance of respective coatings and their ability to perform under cutting in harsh conditions. Harsh conditions are referred where thrust forces are respectively higher with others. Better performance of cutting tool coating is linked with similar stiffness and better adhesion between substrate and coating materials. The thicker coating provides higher edge roundness [52]. This can also be observed that an inclination of 30° provided highest thrust forces for both 7315 and 7325 grades. As per literature [15], better adhesion between substrate and coating materials resulted in better performance. Another reason for better performance is comparable stiffness of both substrate and coating materials.

Figure 21 reports the thrust forces observed for both of the KC7315 and KC7325 drill grades. It can be seen that thrust force was found 20–30% less in the case of KC7325 grade

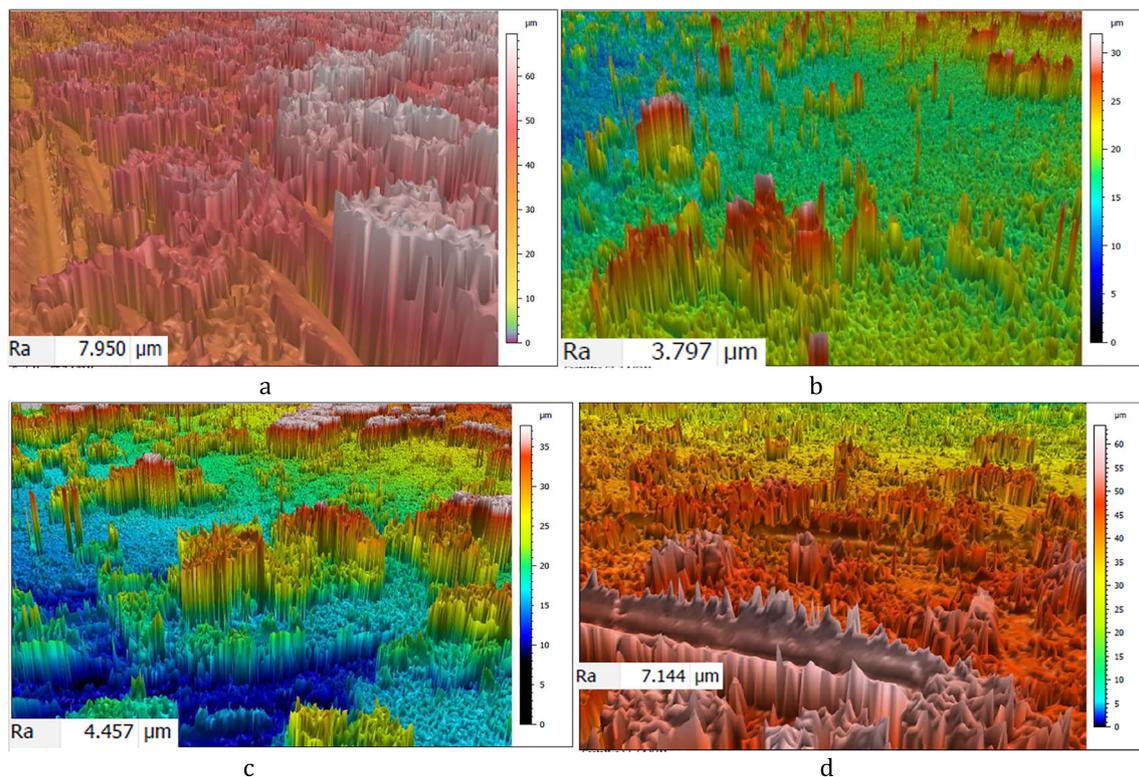


**Fig. 19** Effect of lubrication for the test condition of  $90^\circ$  inclination at 45 m/min, 0.05 mm/rev using 7315 grade tool. (a) Dry cutting. (b) MQL. (c) Compressed air. (d) Flood

(double coated with TiN top layer). Figure 22 reports the 3D confocal surface analyses of surfaces drilled using both drill grades. It can be clearly observed that KC7325 grade (double coated with TiN top layer) provided uniform in-plane fiber cut as compared with the KC7315 grade (with PVD TiAlN coating). Similarly, less fiber pullout, interlaminar delamination, and uncut fiber length were observed with KC7325 grade (double coated with TiN top layer).

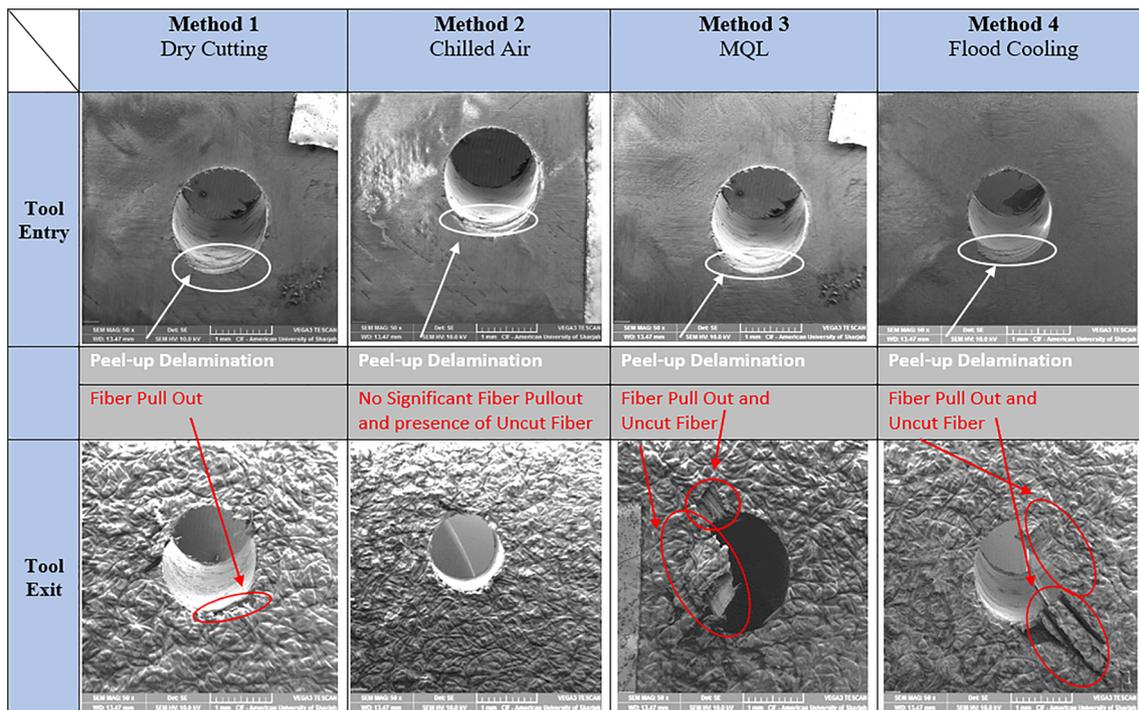
Comparatively lower performance of KC7315 (with PVD TiAlN coating) can be linked with forceful rubbing action of the abrasive nature of carbon fiber. Literature also points out at the poor wear resistance of TiAlN-coated carbide tools due to their vulnerability to oxidation [44]. In order to see the influence of cutting tool material coatings, few drilling tests were conducted using uncoated, KC7315 grade (with PVD TiAlN coating) and KC7325 grade (double coated with TiN top layer) twist drills with similar geometry. The SEM of resulting tests are reported in Fig. 23. It can be observed that KC 7325 grade (double coated with TiN top layer) provided the comparatively higher entry delamination.

#### 4.4 Effect of process parameters

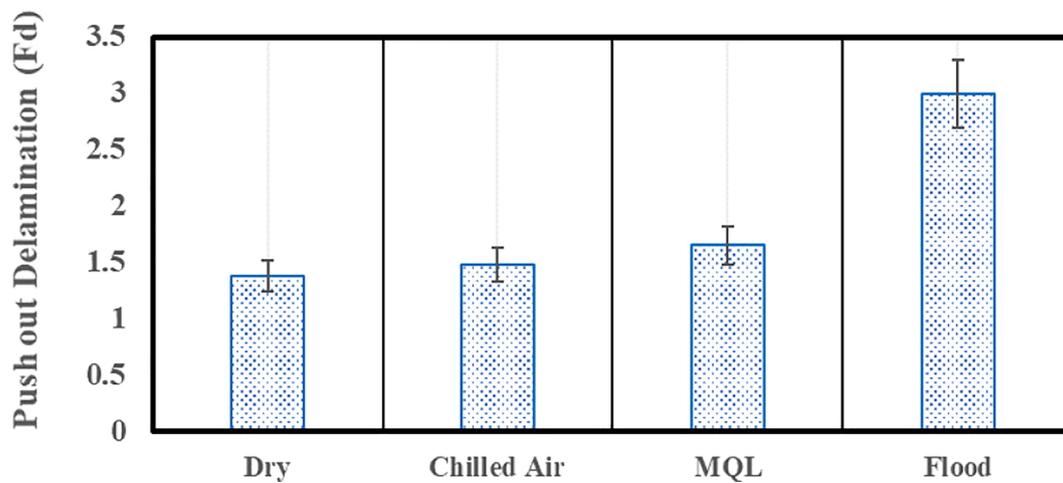
To investigate the relationship between thrust force and the cutting parameters sample condition of  $60^\circ$  inclination

under MQL cooling has been reported in Fig. 24. The relationship of average thrust force with respect to two levels of feed rate and cutting speed were plotted as shown in Fig. 24a and b. It has been observed that when cutting speed was increased from 25 to 35 m/min, thrust force lowers by approximately 20%. Higher cutting speeds generally results in the cutting action with higher cutting temperature. Higher cutting temperature can easily exceed glass transition temperature of the resin-matrix to lower soften it. Literature also points out at the similar trends [53]. Due to this softening of matrix, thrust force can become lower. However, it has been observed that variation in feed rate from 250 mm/min to 500 mm/min slightly increased the thrust force by 7–8%. A possible reason of this slight increase can be due to the low thickness of the CFRP plate utilized for the current work. Due to which, matrix softening was not significant, and elastic recovery of broken fibers dominated to provide slightly higher cutting force.

Figure 25a and b represents the 3D confocal surface analysis of holes drilled at the cutting speeds of 25/min and 65/min, respectively. Higher cutting speed generated cutting action that results in the uniform fiber cutting as can be observed in Fig. 26b. Both Fig. 25a and b show the presence of uncut fiber length, fiber fracture mode I, and delamination. The



a



b

**Fig. 20** **a** KC 7315 grade cutting tool for entry and exit profiles when drilled at 60° inclination angle. **b** Delamination factor calculated for push-out delamination at exit

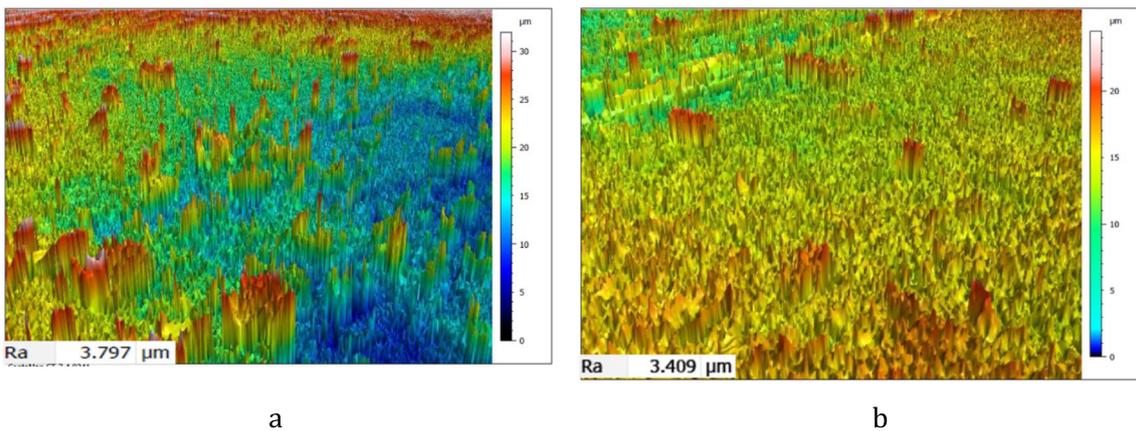
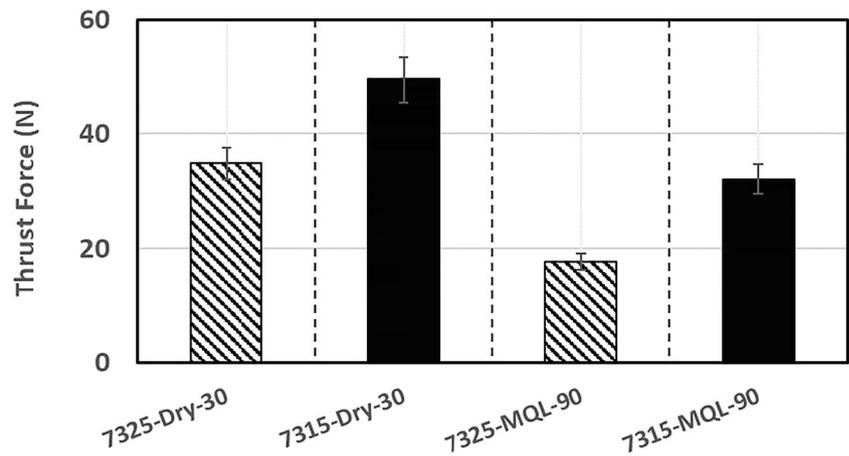
roughness value was also found lower at higher cutting speed of 65 m/min (3.944  $\mu\text{m}$ ) as compared with the cutting speed of 25 m/min (4.516  $\mu\text{m}$ ).

Figure 26a and b represents the 3D confocal surface analysis of holes drilled at the feed rates of 750 mm/min and 1000 mm/min, respectively. Higher feed rate means that main cutting edge will exert more cutting pressure in the downward and circumferential directions. This cutting action can be

observed easily on Fig. 26b as compared with Fig. 26a. Higher surface roughness of 4.716  $\mu\text{m}$  was observed for the feed rate of 1000 mm/min as compared with the 3.998  $\mu\text{m}$  for feed rate of 750 mm/min. Higher percentage of fiber pullout, uncut fiber, and mode I fiber fracture can be noticed in Fig. 26b.

As observed in Fig. 27 SEM micrographs, increase in delamination was reported in the form of breaking out. The SEM

**Fig. 21** Influence of cutting tool material using cutting speed of 45 m/min and feed rate of 250 m/min

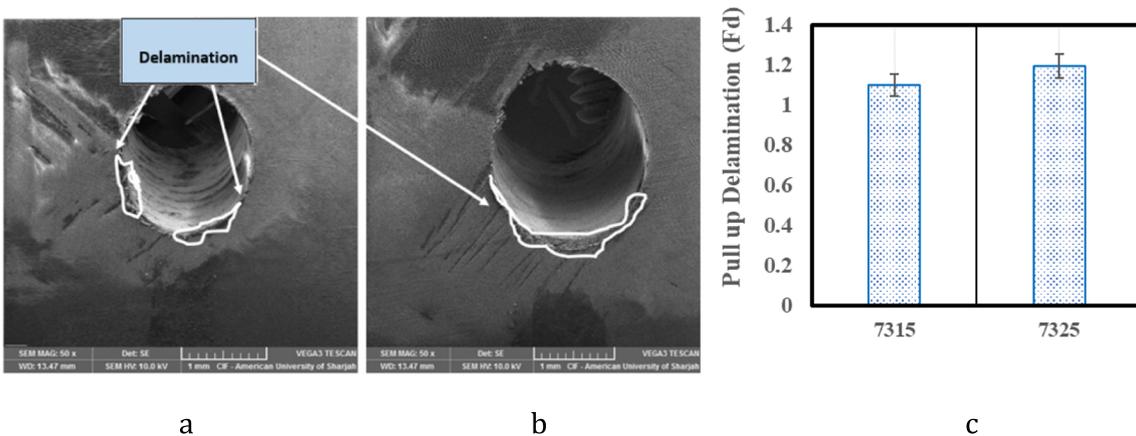


**Fig. 22** 3D Surface roughness of CFRP when drilling 45 m/min, 1000 mm/min, Dry Cut, 30°

observations were found in accordance with the thrust forces reported in earlier section.

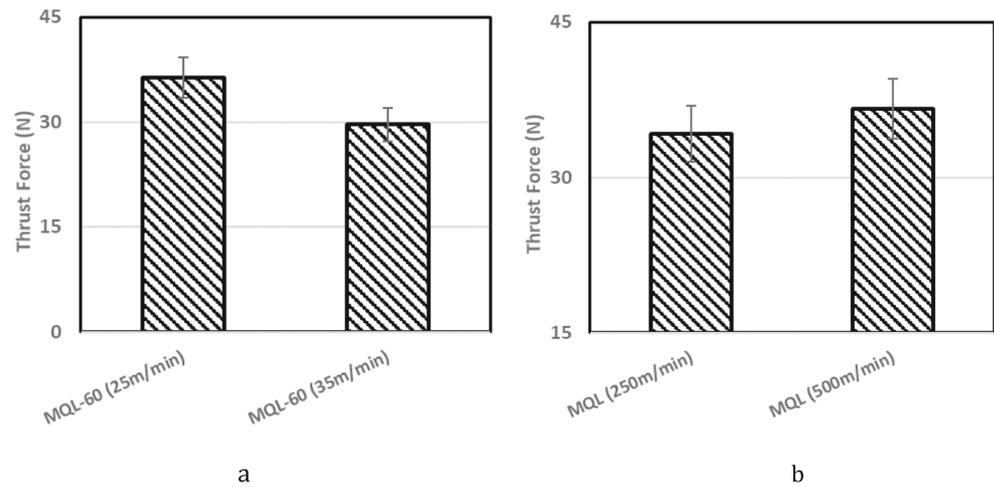
The SEM for different drilling test conducted at different speeds were reported in the Fig. 28. The results

revealed that breakout delamination at entry condition was evident when drilling was performed at low cutting speeds. It can be due to the presence of high thrust force as discussed earlier. However, higher cutting speed can



**Fig. 23** Entry profiles when drilled at inclination angle of 60° under dry lubrication. (a) KC 7315. (b) KC 7325. (c) Hole entry-pull out delamination

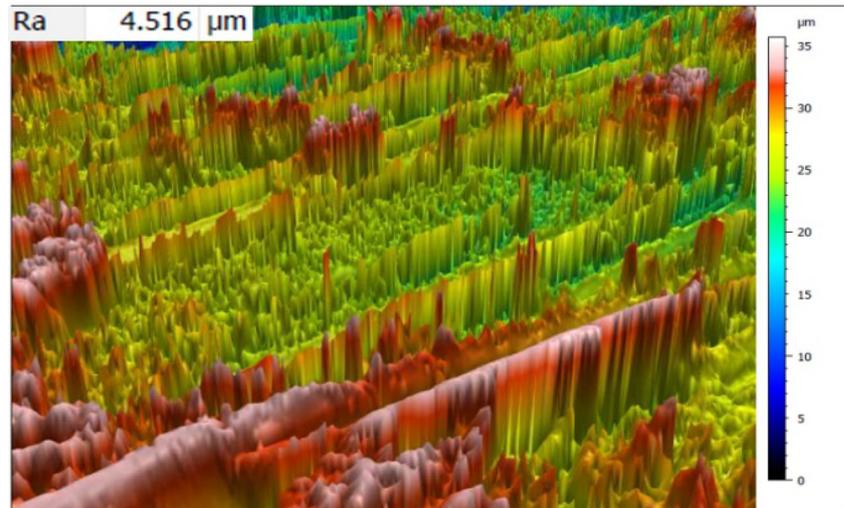
**Fig. 24** Influence of cutting speed and feed rate under MQL lubrication for the cutting tool of KC 7325 (a) Effect of cutting speed at feed rate of 250 m/min (b) Effect of feed rate at cutting speed of 45 m/min



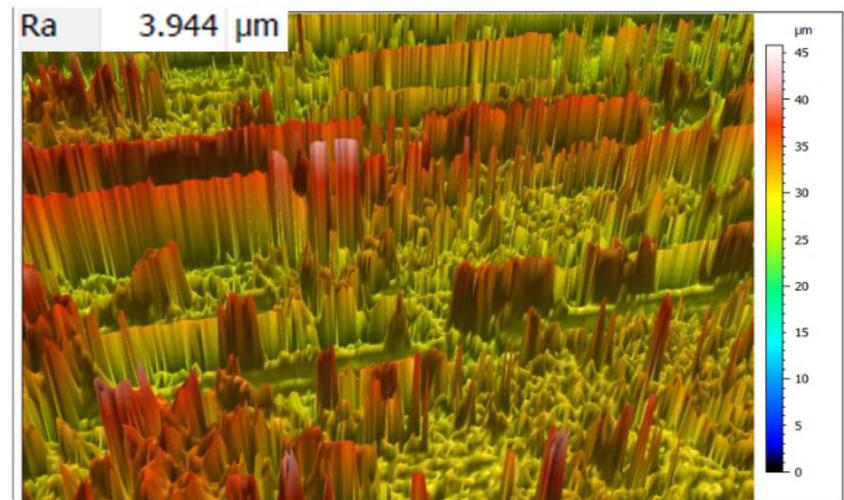
make the initial penetration easier due to low thrust force for drill and can result in the delamination as observed in

Fig. 28a and b. Similar behavior was reported in the existing CFRP drilling literature [23, 24, 26].

**Fig. 25** Effect of cutting speed for feed rate (1000 mm/min), Dry Cut, 30°, tool KC7325 grade. (a) 25 m/min and (b) 65 m/min



a



b

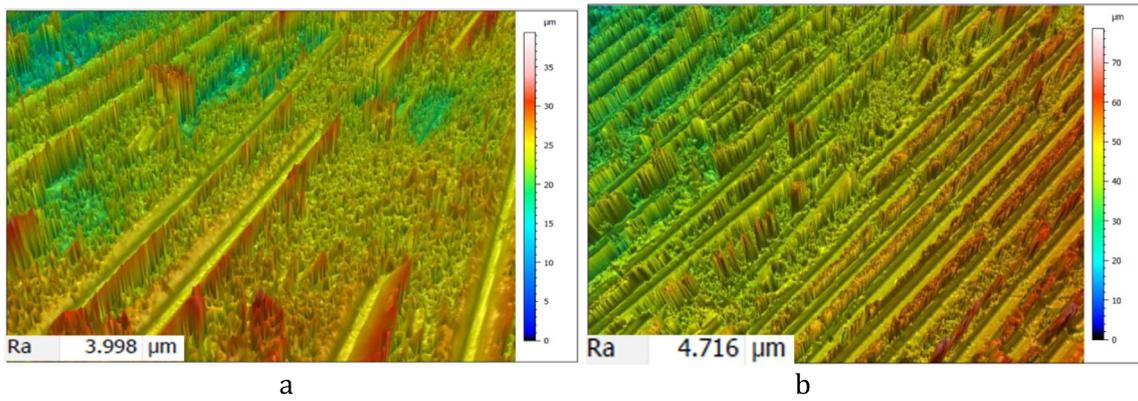


Fig. 26 Effect of feed rate 45 m/min, dry cut, 30°, and tool KC7325 grade. (a) 750 mm/min and (b) 1000 mm/min

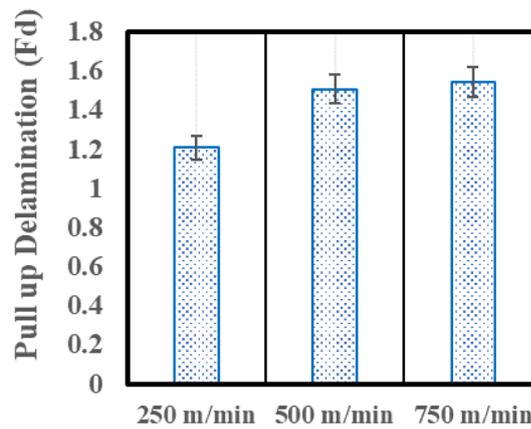
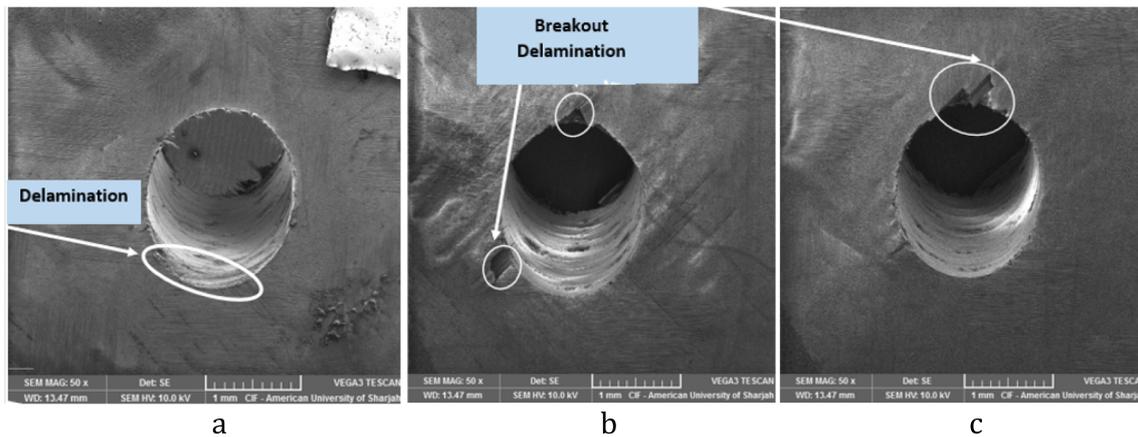
### 5 Conclusions

The following conclusions can be drawn from the current experimental work on sustainable inclined drilling of CFRP.

- In dry cutting, thrust forces were found 2.38 times higher in the 30° inclination when compared with the reference

90° conventional inclination angle. For 30° inclination, compressed air provided lowest increase (1.46 times) in the thrust forces.

- The thrust force reported against both cutting tools exposed that 7325 grade (TiN top coating) generated lower thrust forces as compared with the 7315 grades (with PVD TiAlN coating). The possible reason of this thrust



d

Fig. 27 Influence of feed rate when drilling at 60° inclination angle using KC 7325 (a) 250 m/min (b) 500 m/min, and (c) 750 m/min (d) pull-up delamination

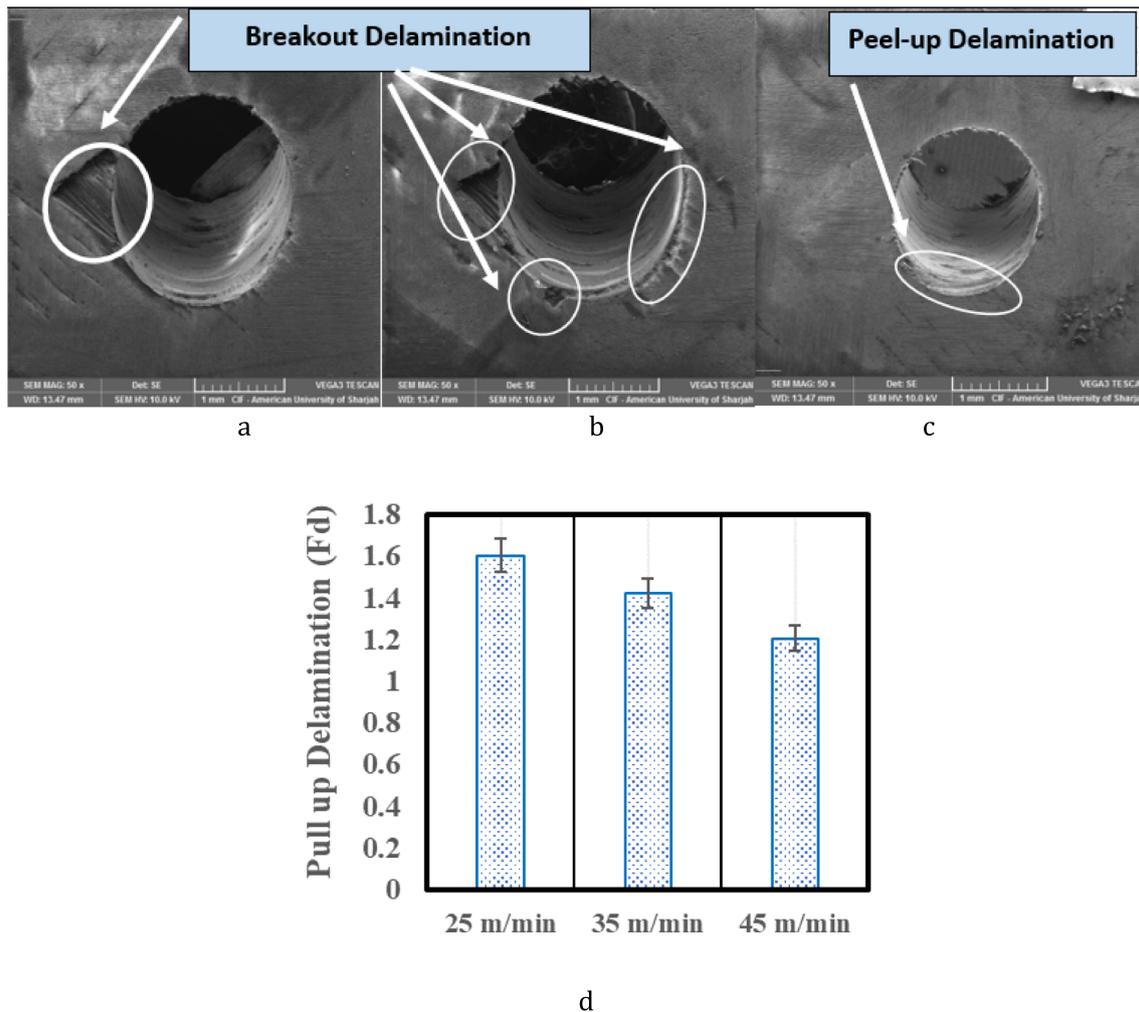


**Fig. 28** Influence of cutting speed when drilling at 60° inclination angle using KC 7325 (a) 25 m/min, (b) 35 m/min, and (c) 45 m min (d) pull\*up delamination

force behavior can be linked with the poor performance of 7315 grade with TiAlN coating. To support the better performance, possible reason could be better adhesion and similar stiffness between substrate and coating materials as mentioned in literature [15].

- Keeping in view that cutting lip indents CFRP laminates initially, 30° inclination angle was the most difficult among other inclinations; as a result the cutting action in this case provided higher magnitudes of the thrust forces. A possible reason of this can be linked to the interaction of drill cutting lips and geometry with the CFRP laminates at the hole entry. In inclined drilling the hole initiation is not cutting CFRP from chisel edge at low angle of 30° inclination angle. However, lowest thrust forces were observed at 90° inclination angle.
- Drilling at higher levels of feed rate provided higher thrust forces and severe delamination with evident plowing marks, more fiber pullout, and fiber fracture mode I at exit delamination. It is linked with the

application of higher pressure at higher feed levels. It means that feed rate should be appropriately selected when drilling at inclination angles.

- Higher breakout delamination was observed at entry for lower cutting speeds representing difficult penetration of tool entry at inclined CFRP surface. It is linked with the presence of higher thrust force at low cutting speed. It has been observed that when cutting speed was increased from 25 to 35 m/min, thrust force lowers by approximately 20%. Higher cutting speeds generally results in the cutting action with higher cutting temperature. Higher cutting temperature can easily exceed glass transition temperature of the resin-matrix to lower soften it.
- In inclined CFRP drilling, MQL and chilled air cutting provided, respectively, controlled fiber pullout, fiber fracture mode I, and fracture mode III out of the plane delamination, whereas dry and flood cooling revealed severe pull-out delamination and the presence of uncut fibers.

- It has been observed that MQL strategy in external configuration did not provide good performance. A possible reason is associated with sub-surface cutting that happens with the MQL-assisted CFRP machining, and lubricant flows into the cavities besides creating a lubrication film.
- The study will open up more specific applications in the aerospace sector especially when CFRP composite is stacked with the titanium or aluminum alloys.

**Acknowledgments** Authors sincerely acknowledge the financial support provided by Dubai Silicon Oasis Authority (DSOA), Rochester Institute of Technology-Dubai (RIT-D), and American University of Sharjah (AUS).

## Appendix

### Specifications of the equipment

**Table 5** Technical specifications of Maxmill VMC (vertical machining center) QMC-850 [54]

Parameters	Value
Table working area	950 × 500 mm
Table maximum loading	500 kg
Spindle speed	10,000 rpm
Spindle cooling system	Oil cooled
Axis motor maximum rating	7.5 kW (10HP)
Feed rate of X, Y, and Z axes	36/36/20 m/min
Positioning accuracy	P0.01 mm
Repeatability accuracy	Ps0.006 mm

**Table 6** Technical specifications of Kistler multi-channel dynamometer 9129AA [55]

Technical data	Value
Measurement range (Fx, Fy, and Fz)	−10 ~ 10 kN
Sensitivity Fx and Fz	≈ −8 pC/N
Sensitivity Fy	≈ −4.1 pC/N
Operating temperature range	0–70 °C
L × W × H	90 × 105 × 32 mm
Weight	3.2 kg
Natural frequency, fn(x)	≈ 3.5 kHz
Natural frequency, fn(y)	≈ 4.5 kHz
Natural frequency, fn(z)	≈ 3.5 kHz

**Table 7** Technical specifications of VEGA 3 Tescan scanning electron microscope [56]

Parameters	Value
Electron gun	Tungsten-heated cathode
Resolution (high vacuum)	3 nm at 30 keV 8 nm at 3 keV
Resolution (low vacuum)	3.5 nm at 30 keV
Chamber-high-vacuum mode	< 9 × 10 <sup>−3</sup> Pa2
Magnification continuous from	3 × − 1,000,000 ×
Electron beam energy	200 eV to 30 keV
Probe current	1 pA to 2 μA
Scanning speed	From 20 ns to 10 ms per pixel adjustable in steps or continuously

**Open Access** This article is licensed under a Creative Commons Attribution 4.0 International License, which permits use, sharing, adaptation, distribution and reproduction in any medium or format, as long as you give appropriate credit to the original author(s) and the source, provide a link to the Creative Commons licence, and indicate if changes were made. The images or other third party material in this article are included in the article's Creative Commons licence, unless indicated otherwise in a credit line to the material. If material is not included in the article's Creative Commons licence and your intended use is not permitted by statutory regulation or exceeds the permitted use, you will need to obtain permission directly from the copyright holder. To view a copy of this licence, visit <http://creativecommons.org/licenses/by/4.0/>.

## References

1. Pervaiz S, Kannan S, Kishawy HA (2018) An extensive review of the water consumption and cutting fluid based sustainability concerns in the metal cutting sector. *J Clean Prod* 197:134–153. <https://doi.org/10.1016/j.jclepro.2018.06.190>
2. Pervaiz S, Anwar S, Qureshi I, Ahmed N (2019) Recent advances in the machining of titanium alloys using minimum quantity lubrication (MQL) based techniques. *Int J Precis Eng Manuf - Green Technol* 6:133–145. <https://doi.org/10.1007/s40684-019-00033-4>
3. Pušavec F, Kopač J (2011) Sustainability assessment: cryogenic machining of iniconel 718. *Stroj Vestnik/Journal Mech Eng* 57: 637–647. <https://doi.org/10.5545/sv-jme.2010.249>
4. Liu DF, Tang YJ, Cong WL (2012) A review of mechanical drilling for composite laminates. *Compos Struct* 94:1265–1279. <https://doi.org/10.1016/j.compstruct.2011.11.024>
5. Xu J, Li C, El Mansori M et al (2018) Study on the frictional heat at tool-work Interface when drilling study on the frictional heat at tool-work Interface when drilling CFRP CFRP costing models capacity in of industry of mechanical optimization between used capacity and PR China efficiency. *Procedia Manuf* 26:415–423. <https://doi.org/10.1016/j.promfg.2018.07.049>
6. Xia T, Kaynak Y, Arvin C, Jawahir IS (2016) Cryogenic cooling-induced process performance and surface integrity in drilling CFRP composite material. *Int J Adv Manuf Technol* 82:605–616. <https://doi.org/10.1007/s00170-015-7284-y>
7. Oluwarotimi S, Nath H, Popov I, Beaugrand J (2016) Engineering Science and Technology, an International Journal Comprehensive

- study on machinability of sustainable and conventional fibre reinforced polymer composites. *Eng Sci Technol an Int J* 19:2043–2052. <https://doi.org/10.1016/j.jestch.2016.07.010>
8. Brinksmeier E, Janssen R (2002) Drilling of multi-layer composite materials consisting of carbon fiber reinforced plastics (CFRP), titanium and aluminum alloys. *CIRP Ann - Manuf Technol* 51: 87–90. [https://doi.org/10.1016/S0007-8506\(07\)61472-3](https://doi.org/10.1016/S0007-8506(07)61472-3)
  9. Senthilkumar M, Prabukarthi A, Krishnaraj V (2018) Machining of CFRP/Ti6Al4V stacks under minimal quantity lubricating condition. *J Mech Sci Technol* 32:3787–3796. <https://doi.org/10.1007/s12206-018-0731-6>
  10. Merino-Pérez JL, Royer R, Ayvar-Soberanis S, Merson E, Hodzic A (2015) On the temperatures developed in CFRP drilling using uncoated wc-co tools part I: Workpiece constituents, cutting speed and heat dissipation. *Compos Struct* 123:161–168. <https://doi.org/10.1016/j.compstruct.2014.12.033>
  11. Meshreki M, Damir A, Sadek A, Attia MH (2016) Investigation of drilling of CFRP-Aluminium stack under different cooling modes. *ASME International Mechanical Engineering Congress and Exposition, In*
  12. Zitoune R, Collombet F (2007) Numerical prediction of the thrust force responsible of delamination during the drilling of the long-fibre composite structures. *Compos Part A Appl Sci Manuf* 38: 858–866. <https://doi.org/10.1016/j.compositesa.2006.07.009>
  13. Gaugel S, Sripathy P, Haeger A, Meinhard D, Bernthaler T, Lissek F, Kaufeld M, Knoblauch V, Schneider G (2016) A comparative study on tool wear and laminate damage in drilling of carbon-fiber reinforced polymers (CFRP). *Compos Struct* 155:173–183. <https://doi.org/10.1016/j.compstruct.2016.08.004>
  14. Schulze V, Becke C, Weidenmann K, Dietrich S (2011) Machining strategies for hole making in composites with minimal workpiece damage by directing the process forces inwards. *J Mater Process Technol* 211:329–338. <https://doi.org/10.1016/j.jmatprotec.2010.10.004>
  15. Swan S, Bin AMS, Kim D et al (2018) Tool wear of advanced coated tools in drilling of CFRP. *J Manuf Sci Eng Trans ASME* 140:140. <https://doi.org/10.1115/1.4040916>
  16. Khashaba UA (2013) Drilling of polymer matrix composites: a review. *J Compos Mater* 47:1817–1832. <https://doi.org/10.3224/zff.v30i2.02>
  17. Xu J, Ji M, Paulo Davim J, Chen M, el Mansori M, Krishnaraj V (2020) Comparative study of minimum quantity lubrication and dry drilling of CFRP/titanium stacks using TiAlN and diamond coated drills. *Compos Struct* 234:111727. <https://doi.org/10.1016/j.compstruct.2019.111727>
  18. Xu J, Huang X, Chen M, Paulo Davim J (2020) Drilling characteristics of carbon/epoxy and carbon/polyimide composites. *Mater Manuf Process* 00:1–9. <https://doi.org/10.1080/10426914.2020.1784935>
  19. Xu J, Huang X, Davim JP et al (2020) On the machining behavior of carbon fiber reinforced polyimide and PEEK thermoplastic composites. *Polym compos* 1–15. <https://doi.org/10.1002/pc.25663>
  20. Xu J, Li C, Chen M, el Mansori M, Ren F (2019) An investigation of drilling high-strength CFRP composites using specialized drills. *Int J Adv Manuf Technol* 103:3425–3442. <https://doi.org/10.1007/s00170-019-03753-8>
  21. Xu J, Li C, Mi S, An Q, Chen M (2018) Study of drilling-induced defects for CFRP composites using new criteria. *Compos Struct* 201:1076–1087. <https://doi.org/10.1016/j.compstruct.2018.06.051>
  22. Xu J, Ji M, Chen M, El Mansori M (2020) Experimental investigation on drilling machinability and hole quality of CFRP/Ti6Al4V stacks under different cooling conditions. *Int J Adv Manuf Technol* 109:1527–1539. <https://doi.org/10.1007/s00170-020-05742-8>
  23. Davim JP, Reis P (2003) Study of delamination in drilling carbon fiber reinforced plastics (CFRP) using design experiments. *Compos Struct* 59:481–487. [https://doi.org/10.1016/S0263-8223\(02\)00257-X](https://doi.org/10.1016/S0263-8223(02)00257-X)
  24. Davim JP, Rubio JC, Abrao AM (2007) A novel approach based on digital image analysis to evaluate the delamination factor after drilling composite laminates. *Compos Sci Technol* 67:1939–1945. <https://doi.org/10.1016/j.compscitech.2006.10.009>
  25. Abrão AM, Rubio JCC, Faria PE, Davim JP (2008) The effect of cutting tool geometry on thrust force and delamination when drilling glass fibre reinforced plastic composite. *Mater Des* 29:508–513. <https://doi.org/10.1016/j.matdes.2007.01.016>
  26. Gaitonde VN, Karnik SR, Rubio JC, Correia AE, Abrão AM, Davim JP (2008) Analysis of parametric influence on delamination in high-speed drilling of carbon fiber reinforced plastic composites. *J Mater Process Technol* 203:431–438. <https://doi.org/10.1016/j.jmatprotec.2007.10.050>
  27. Campos Rubio J, Abrao AM, Faria PE, Correia AE, Davim JP (2008) Effects of high speed in the drilling of glass fibre reinforced plastic: evaluation of the delamination factor. *Int J Mach Tools Manuf* 48:715–720. <https://doi.org/10.1016/j.ijmactools.2007.10.015>
  28. Davim JP, Reis P, António CC (2004) Experimental study of drilling glass fiber reinforced plastics (GFRP) manufactured by hand lay-up. *Compos Sci Technol* 64:289–297. [https://doi.org/10.1016/S0266-3538\(03\)00253-7](https://doi.org/10.1016/S0266-3538(03)00253-7)
  29. Langella A, Nele L, Maio A (2005) A torque and thrust prediction model for drilling of composite materials. *Compos Part A Appl Sci Manuf* 36:83–93. <https://doi.org/10.1016/j.compositesa.2004.06.024>
  30. Merchant ME (1945) Mechanics of the metal cutting process. *J Appl Phys* 16:267–275
  31. Li H, Qin X, He G, Price MA, Jin Y, Sun D (2017) An energy based force prediction method for UD-CFRP orthogonal machining. *Compos Struct* 159:34–43. <https://doi.org/10.1016/j.compstruct.2016.09.051>
  32. Chandrasekharan V, Kapoor SG, DeVor RE (1995) A mechanistic approach to predicting the cutting forces in drilling : with application to fiber-reinforced composite materials. *J Eng Ind* 117:559–570
  33. Yan X, Zhang K, Cheng H, Luo B, Hou G (2019) Force coefficient prediction for drilling of UD-CFRP based on FEM simulation of orthogonal cutting. *Int J Adv Manuf Technol* 104:3695–3716
  34. Ramulu M, Kim D, Choi G (2003) Frequency analysis and characterization in orthogonal cutting of glass fiber reinforced composites. *Compos Part A Appl Sci Manuf* 34:949–962. [https://doi.org/10.1016/S1359-835X\(03\)00203-3](https://doi.org/10.1016/S1359-835X(03)00203-3)
  35. Khashaba UA, Selmy AI, Megahed AA (2010) Composites : part a machinability analysis in drilling woven GFR / epoxy composites : part I – effect of machining parameters. *Compos Part A* 41:391–400. <https://doi.org/10.1016/j.compositesa.2009.11.006>
  36. Hocheng H, Tsao CC (2005) The path towards delamination-free drilling of composite materials 167:251–264 . <https://doi.org/10.1016/j.jmatprotec.2005.06.039>
  37. Su F, Zheng L, Sun F, Wang Z, Deng Z, Qiu X (2018) Novel drill bit based on the step-control scheme for reducing the CFRP delamination. *J Mater Process Technol* 262:157–167. <https://doi.org/10.1016/j.jmatprotec.2018.06.037>
  38. Garrett JD (2016) Experimentation of mode I & mode II fracture of Uni-directional composites and finite element analysis of mode I fracture using cohesive contact
  39. Sreejith PS, Krishnamurthy R, Malhotra SK, Narayanasamy K (2000) Evaluation of PCD tool performance during machining of carbon/phenolic ablative composites. *J Mater Process Technol* 104: 53–58. [https://doi.org/10.1016/S0924-0136\(00\)00549-5](https://doi.org/10.1016/S0924-0136(00)00549-5)
  40. Che D, Saxena I, Han P, Guo P, Ehmann KF (2014) Machining of carbon Fiber reinforced plastics/polymers: a literature review. *J Manuf Sci Eng* 136:034001. <https://doi.org/10.1115/1.4026526>

41. Bonnet C, Poulachon G, Rech J, Girard Y, Costes JP (2015) CFRP drilling: fundamental study of local feed force and consequences on hole exit damage. *Int J Mach Tools Manuf* 94:57–64. <https://doi.org/10.1016/j.ijmachtools.2015.04.006>
42. Hintze W, Hartmann D (2013) Modeling of delamination during milling of unidirectional CFRP. *Procedia CIRP* 8:444–449. <https://doi.org/10.1016/j.procir.2013.06.131>
43. Uhlmann E, Richarz S, Sammler F, Hufschmied R (2016) High speed cutting of carbon fibre reinforced plastics. *Procedia Manuf* 6:113–123. <https://doi.org/10.1016/j.promfg.2016.11.015>
44. Wang DHH, Ramulu M, Arola D (1995) Orthogonal cutting mechanisms of graphite/epoxy composite. Part I: unidirectional laminate. *Int J Mach Tools Manuf* 35:1623–1638. [https://doi.org/10.1016/0890-6955\(95\)00014-O](https://doi.org/10.1016/0890-6955(95)00014-O)
45. Lopresto V, Caggiano A, Teti R (2016) High performance cutting of fibre reinforced plastic composite materials. *Procedia CIRP* 46:71–82. <https://doi.org/10.1016/j.procir.2016.05.079>
46. Xu J, An Q, Chen M (2017) An experimental investigation on cutting-induced damage when drilling high-strength T800S/250F carbon fiber-reinforced polymer. *Proc Inst Mech Eng Part B J Eng Manuf* 231:1931–1940. <https://doi.org/10.1177/0954405415619348>
47. Ning F, Wang H, Cong W, Fernando PKSC (2017) A mechanistic ultrasonic vibration amplitude model during rotary ultrasonic machining of CFRP composites. *Ultrasonics* 76:44–51. <https://doi.org/10.1016/j.ultras.2016.12.012>
48. Fu R, Jia Z, Wang F, Jin Y, Sun D, Yang L, Cheng D (2018) Drill-exit temperature characteristics in drilling of UD and MD CFRP composites based on infrared thermography. *Int J Mach Tools Manuf* 135:24–37. <https://doi.org/10.1016/j.ijmachtools.2018.08.002>
49. Ramirez C, Poulachon G, Rossi F, M'Saoubi R (2014) Tool wear monitoring and hole surface quality during CFRP drilling. *Procedia CIRP* 13:163–168. <https://doi.org/10.1016/j.procir.2014.04.028>
50. Ramulu M, Branson T, Kim D (2001) A study on the drilling of composite and titanium stacks. *Compos Struct* 54:67–77. [https://doi.org/10.1016/S0263-8223\(01\)00071-X](https://doi.org/10.1016/S0263-8223(01)00071-X)
51. Durão L, Tavares J, de Albuquerque V, Marques J, Andrade O (2014) Drilling damage in composite material. *Materials (Basel)* 7:3802–3819. <https://doi.org/10.3390/ma7053802>
52. Wang X, Kwon PY, Sturtevant C, Kim D(DW), Lantrip J (2013) Tool wear of coated drills in drilling CFRP. *J Manuf Process* 15:87–95. <https://doi.org/10.1016/j.jmapro.2012.09.019>
53. Campos Rubio JC, Abrão AM, Eustáquio Faria P, Correia AE, Davim JP (2008) Delamination in high speed drilling of carbon fiber reinforced plastic (CFRP). *J Compos Mater* 42:1523–1532. <https://doi.org/10.1177/0021998308092205>
54. MaxMill-CNC (2018) CNC-Milling-Machine. <http://www.maxmill-cnc.com.tw/CNC-Milling-Machine.html>
55. Kistler (2018) Kistler product catalogue: sensors and solutions for cutting force measurement. <https://www.kistler.com/fileadmin/files/divisions/sensor-technology/cutting-force/960-002e-05.14.pdf>
56. TESCAN (2018) 3rd Generation of VEGA SEMs. <https://www.tescan.com/Tescan/media/content/pdf/technology/VEGA3-brochure.pdf?ext=.pdf>

**Publisher's note** Springer Nature remains neutral with regard to jurisdictional claims in published maps and institutional affiliations.